DOI: 10.1070/RCR4601

Radionuclides emitting short-range particles and modular nanotransporters for their delivery to target cancer cells

Alexander S. Sobolev,[a, b] Ramiz A. Aliev,[c, d] Stepan N. Kalmykov [c, d]

[a] *Institute of Gene Biology of the Russian Academy of Sciences*
ul. Vavilova 34/5, 119334 Moscow, Russian Federation
[b] *Department of Biology, Moscow State University*
Leninskie Gory 1, str. 12, 119991 Moscow, Russian Federation
[c] *National Research Centre 'Kurchatov Institute'*
pl. Akademika Kurchatova 1, 123182 Moscow, Russian Federation
[d] *Department of Chemistry, Moscow State University*
Leninskie Gory 1, str. 3, 119991 Moscow, Russian Federation

The survey considers radionuclides emitting short-range particles. Methods for the production of most promising α- and Auger electron emitters and their applications in nuclear medicine are discussed. Most Auger electron emitters can be produced using ordinary cyclotrons that accelerate protons to energies of 15 or 30 MeV. The production of α-emitters is still associated with serious challenges, which hinder their introduction into clinical practice. The main types of vehicles for radionuclide delivery to tumour cells are discussed. The focus is on modular nanotransporters, as the highest cytotoxic effect of ionizing radiation is achieved when radionuclides are complexed with these vehicles. The use of modular nanotransporters will disclose the potentials of many radionuclides that have not so far been regarded as therapeutic agents, specifically ^{67}Ga, ^{111}In and some other.
The bibliography includes 197 references.

Contents

I.	Introduction	1012
II.	Characteristics of Auger electron emitters that show a potential for medical applications	1012
III.	Production of some Auger electron emitters	1013
IV.	Characteristics of α-emitters that show a potential for medical applications	1018
V.	Production of medical α-emitters	1019
VI.	Production facilities	1021
VII.	Main families of delivery vehicles for radionuclides that emit short-range particles	1022
VIII.	Modular nanotransporters: design and properties	1023
IX.	Modular nanotransporters as vehicles for the targeted nuclear delivery of α-particles and Auger electron emitters into target cells	1025
X.	Conclusion	1028

A.S.Sobolev. Doctor of Biological Sciences (habil.), Professor, Head of the Laboratory of Molecular Genetics of Intracellular Transport at the IGB RAS, Professor of the Biophysics Division at the Department of Biology, MSU.
Telephone: +7(499)135 – 3100, E-mail: sobolev@igb.ac.ru
Current research interests: nanomedicine, targeted intracellular delivery of biologically active compounds.
R.A.Aliev. PhD, Vice-head of the Division of Nuclear Medicine of NRC 'Kurchatov Institute', Leading Researcher at the Department of Chemistry, MSU. E-mail: ramiz.aliev@gmail.com
Current research interests: production, separation and preconcentration of radionuclides, radiochemistry.
S.N.Kalmykov. Doctor of Chemical Sciences (habil.), Professor, Head of the Nuclear and Radiation Medicine Section at the NRC 'Kurchatov Institute', Head of the Division of Radiochemistry at the Department of Chemistry, MSU. E-mail: stepan@radio.chem.msu.ru
Current research interests: radiochemistry, radiopharmaceutical chemistry, nuclear fuel cycles, environmental behaviour of radionuclides, separation and preconcentration of radionuclides.

Received 9 October 2015
Translation: O.P.Fedorova

© 2016 Russian Academy of Sciences and Turpion Ltd.

I. Introduction

It was almost 90 years ago, in 1927, that Regaud and Lacassagne,[1] famous French radiologists, described the desired anticancer agent as follows. An ideal agent for cancer therapy would consist of heavy elements capable of emitting radiations of molecular dimensions, which could be administered to the organism and selectively fixed in the protoplasm of cells one seeks to destroy. Many contemporary researchers have come to the conclusion that this ideal is satisfied to a greatest extent by radionuclides that emit short-range particles and are delivered into cancer cell nuclei, as their damaging effect extends to a distance commensurate with the sizes of molecules or cells, thereby minimizing the damage of surrounding normal cells and tissues.[2–6] The radionuclides emitting particles that have short ranges and high linear energy transfer (LET) values are regarded to be especially suitable for the purpose of treatment of small and disseminated tumours.[7] In general, isotopes that have half-lives close to the characteristic existence times of their vehicles (for example, antibodies or their labelled fragments) in cancer cells, short ranges (up to several tens of cell diameters) and good opportunities for production and loading on vehicles were regarded to be optimal radionuclides for therapeutic purposes.[8–10]

Only few targeted anticancer radiopharmaceuticals (RPs) are now allowed for therapeutic use. These are Zevalin® (Spectrum Pharmaceuticals, USA) and Bexxar® (GlaxoSmithKline, USA), which are monoclonal antibodies against antigen CD20 labelled by β-emitters ^{90}Y and ^{131}I, respectively, intended for the treatment of B-cell lymphoma. Recently (in May, 2013), the Food and Drug Administration of the USA gave permission for the clinical use of Xofigo® (previously named Alpharadin; Algeta, Norway, then Bayer, Germany), radium-223 chloride, for the treatment of bone metastases in patients with castration-resistant prostate cancer.[11–14] This is an exclusive case of today's application of a radionuclide salt without special delivery vectors, as it has a pronounced affinity to bone tissue.[15]

Many pharmaceuticals are now in various phases of clinical studies. The peptide agent labelled with ^{213}Bi (^{213}Bi-DOTA-Substance P) (DOTA stands for 1,4,7,10-tetraazacyclododecane-1,4,7,10-tetraacetic acid) was found to have a therapeutic effect against glioblastoma and glioma.[16, 17] The ^{213}Bi-DOTA-Substance P therapy was shown to significantly increase the average life-time both in glioblastoma patients (studied in 24 patients) and in glioma patients (studied in six patients) in combination with surgical treatment, chemotherapy and radiation therapy. The highest therapeutic effect is attained by several consecutive applications using an agent that has a total activity of up to 11 GBq.

In 2014, Kratochwil *et al.*[18] published the results of two-year clinical trials of a peptide pharmaceutical, an analogue of somatostatin loaded with ^{213}Bi (^{213}Bi-DOTATOC), for the therapy of neuroendocrine liver metastases (seven patients) and bone marrow carcinomatosis (one patient) that were resistant to β-emitting RPs (^{90}Y-DOTATOC and ^{177}Lu-DOTATOC). (For more details of the clinical trials of α-emitting radiopharmaceuticals, see Section VII.)

Some delivery vehicles for medical short-range radionuclides are described in surveys that were published in the last five years.[5, 7, 19–24] Our survey is focused on modular nanotransporters as delivery vehicles for a very wide range of radionuclides and biologically active compounds in general.

II. Characteristics of Auger electron emitters that show a potential for medical applications

Nuclear decay *via* electron capture or conversion electron emission generates an atom with a vacancy in the inner shell. Electron redistribution over shells leads to the emission of an Auger cascade. Electron capture and conversion electron emission can occur consecutively. For example, the electron capture decay of ^{125}I is followed by the emission of Auger cascade. The decay results in the ^{125}*Te daughter nucleus, which then enters the ground state with conversion electron emission to generate a new Auger cascade. The atom can loss up to tens of electrons as a result.

The DNA damaging effect of ^{125}I, which considerably exceeds the effect expected from its γ-emission, has long been known.[25–27] This effect could likewise be assigned to transmutation (conversion to ^{125} Te as a result of electron capture), to the effect of recoil nuclei, or to Auger effects. Later experiments using ^{125}I-labelled compounds that penetrated cellular nuclei but did not enter nuclear DNA [28] made it possible to recognize the Auger electron effects and elucidate their prominent cytotoxic activity. Convincing experimental evidence was obtained that the DNA is just the target whose damage by Auger electrons leads to the death of the cell.[29] The yields of various damages caused in DNA by Auger electrons emitted by various radionuclides are listed in Table 1. In this context, one should keep in mind that, in one decay, only a small volume (on the order of several cubic nanometers) around the decaying atom receives a considerable dose,[31] of about 10^4 – 10^7 Gy, because of the short range and the high LET of Auger electrons (Table 2).

The DNA-damaging efficacy depends on the distance between the atom emitting Auger electrons (Auger emitter) and the DNA. This dependence was shown experimentally using ^{125}I-iodinated derivatives of a DNA-intercalator (Hoechst 33258 dye) that had different chain lengths and, accordingly, different distances between the ^{125}I atom and DNA.[33]

For many Auger electron emitters, absorbed doses per unit cumulated radioactivity (*S*) were calculated for the cellular nucleus as a target depending on the emitter location, for example, in the nucleus (N) or on the cell surface (CS).[34] Table 3 shows exemplary calculations and *S* ratios for two cases (N ← N and N ← CS) to compare the effects of Auger emitters that reside on the cell surface and

Table 1. DNA damage yields for ^{125}I, ^{119}Sb, ^{123}I, ^{111}In and ^{99m}Tc radionuclides.[30]

DNA damage types	Damage yield per billion base pairs and per Gray				
	^{125}I	^{119}Sb	^{123}I	^{111}In	^{99m}Tc
Base damage	7.64	5.73	4.11	3.79	2.18
All types of one-strand breaks	4.62	3.59	2.50	2.33	1.43
All types of two-strand breaks	0.38	0.31	0.21	0.20	0.13

Table 2. Characteristics of Auger electron emitters of medical importance.[31, 32]

Radionuclide	Average Auger electron number per decay	General yield of electrons with various ranges per decay (%)		
		< 0.5 μm	< 100 nm	< 2 nm
^{125}I	20	98	86	39
^{123}I	11	98	89	40
^{77}Br	7	100	95	51
^{111}In	15	98	91	53
^{193m}Pt	30	97	93	21
^{195m}Pt	36	92	79	19
LET /keV μm^{-1}		4 – 26	9 – 26	< 18

Table 3. Absorbed dose per unit cumulated radioactivity for selected Auger electron emitters.[35]

Radionuclide	S/Gy Bq^{-1} s^{-1}		S(N ← N) : S(N ← CS)
	N ← N	N ← CS	
^{67}Ga	1.88×10^{-3}	3.30×10^{-5}	56.4
^{99m}Tc	8.16×10^{-4}	1.38×10^{-5}	59.1
^{111}In	1.47×10^{-3}	7.29×10^{-5}	20.2
^{203}Pb	2.67×10^{-3}	1.62×10^{-5}	164.8
^{125}I	3.51×10^{-3}	1.18×10^{-4}	29.7
^{123}I	1.56×10^{-3}	6.28×10^{-5}	24.8

Note. Here and in Table 7, the cell has a diameter of 16 μm and the nucleus has a diameter of 10 μm; variants are considered where the target is the nucleus and the source is the nucleus (N ← N), or the target is the nucleus and the source is the cell surface (N ← CS), and their ratios.

inside the cell nucleus. The data of Table 3 imply the feasibility of delivering Auger emitters into the nuclei of target cells in order to achieve their highest cytotoxicities.

Auger emitters are, as a rule, neutron-deficient nuclides and, therefore, they can be produced on accelerators that accelerate positively charged particles. The Auger effect allows one to look in a new way at the long-known and widely used radionuclides. So, provided suitable delivery vehicles are used, any one of ^{99m}Tc, ^{123}I, ^{124}I and ^{111}In can turn from a diagnostic tool to a therapeutic nuclide. In other words, the range of potential therapeutic Auger emitters to a great deal overlaps with the range of nuclides currently used for single photon emission computed tomography (SPECT) and positron emission tomography (PET), for which production facilities have already been created and routes for incorporation into biomolecules have been developed.

In order for an Auger emitter to find medical application, it should meet the following requirements as fully as possible; that is, this Auger emitter should:

— decay *via* electron capture or isomeric transition;

— have a half-life ($T_{1/2}$) in the range from several hours to several days;

— decay to a stable or long-lived nuclide;

— have no strong hard γ-lines;

— have chemical properties that provide for firm binding to the vehicle; and

Table 4. Key nuclear properties of candidate Auger therapeutic nuclides.[36]

Nuclide	$T_{1/2}$	Decay type [a]
^{67}Ga	3.26 days	EC
^{77}Br	2.38 days	EC
^{99m}Tc	6.01 h	IT
^{111}In	2.80 days	EC
^{119}Sb	1.59 days	EC
^{123}I	13.27 h	EC
^{124}I	4.18 days	EC, β+
^{140}Nd	3.37 days	EC, β+
^{165}Er	10.36 h	EC
^{167}Tm	9.25 days	EC
^{191}Pt	2.96 days	EC
^{193m}Pt	4.33 days	IT
^{195m}Pt	4.02 days	IT
^{201}Tl	3.04 days	EC
^{203}Pb	2.16 days	EC

[a] EC stands for electron capture; IT stands for isomeric transition.

— be produced by facile routes, preferably by ordinary types of cyclotrons.

There are many radionuclides that meet the above requirements to some degree; the major candidates are listed in Table 4.

III. Production of some Auger electron emitters

As a rule, there are several routes to produce one and the same radionuclide. In choosing the optimal route, one should take into account the following criteria:

— availability of an appropriate accelerator;

— availability of the target material;

— yield and radionuclide purity requirements;

— desired specific activity; and

— difficulty of chemical separation.

Table 5 lists the main routes to produce Auger emitters, the yields of the relevant nuclear reactions and major impurities. Some pieces of data are theoretical quantities derived from experimentally determined cross sections; other pieces were obtained from experiments, where the result was impacted by the radiation loss of matter, isotopic impurities in the target and other factors.

III.1. Gallium-67

Gallium-67 is widely used for SPECT diagnosis and is now regarded to be a promising therapeutic Auger emitter; its production methods are well developed. Gallium-67 is formed by the reaction ^{68}Zn(p,2n)^{67}Ga with a cross section (σ_{max}) of ~720 mbarn at 20 – 21 MeV.[36] The most important by-product [^{66}Ga (9.49 h) †] is produced by the reaction ^{68}Zn(p,3n)^{66}Ga starting at about 25 MeV; the yield at 30 MeV is ~22 MBq A^{-1} h^{-1} (Ref. 38).

The reaction ^{67}Zn(p,n)^{67}Ga is of less importance because of the low ^{67}Zn abundance in the natural mixture (4.7%), despite a comparable value of $\sigma_{max} \approx 610$ mbarn at 10 – 11 MeV.[37]

† Hereafter, the parenthesized figure having the dimension of time following the nuclide symbol denotes the nuclide half-life.

Table 5. Production of Auger electron emitters for targeted radiotherapy.

Nuclide	Production route	Energy /MeV	Yield /MBq μA^{-1} h^{-1}	Most important impurities [content (%)] [a]	Ref.
^{67}Ga	^{67}Zn(p,n)^{67}Ga	15 → 0	87	–	37
	^{68}Zn(p,2n)^{67}Ga	30 → 13	300	^{66}Ga (7)	37, 38
	^{nat}Zn(d,*x*n)^{67}Ga	23 → 2	18	^{66}Ga (> 1000)	39
	^{66}Zn(d,n)^{67}Ga	11 → 2	30	–	39
^{77}Br	^{77}Se(p,n)^{77}Br	14 → 0	100	–	40
	^{78}Se(p,2n)^{77}Br	25 → 15	220	–	40
	^{nat}Se(p,*x*n)^{77}Br	25 → 15	73	^{76}Br (145), ^{82}Br (3)	41
	^{75}As(α,2n)^{77}Br	28 → 14	3.3 [b]	–	42
			14		40
^{99m}Tc	^{100}Mo(p,2n)^{99m}Tc	18 → 10	500	^{99g}Tc	43
	^{96}Zr(α,n)^{99}Mo → ^{99m}Tc	30 → 0	1.6 (^{99}Mo)	–	44
^{111}In	^{111}Cd(p,n)^{111}In	15 → 0	72	–	37
	^{112}Cd(p,2n)^{111}In	30 → 11	311	–	37
	^{nat}Ag(α,*x*n)^{111}In	38 → 0	11	–	45
^{119}Sb	^{119}Sn(p,n)^{119}Sb	15 → 0	150	^{120m}Sb (> 0.023)	46, 47
^{123}I	^{124}Xe(p,2n)^{123}Cs → ^{123}Xe → ^{123}I (^{124}Xe(p,pn)^{123}Xe → ^{123}I)	29 → 23	414 [c]	–	48
	^{123}Te(p,n)^{123}I	18 → 8	302	–	37
	^{124}Te(p,2n)^{123}I	25 → 18	791	^{124}I (0.9)	37
^{124}I	^{124}Te(p,n)^{124}I	12 → 8	16	^{123}I (1), ^{125}I (< 0.1)	49
		11 → 0	8.5 [d]	–	50
	^{125}Te(p,2n)^{124}I	21 → 15	81	^{123}I (7.4) ^{125}I (0.9)	51
	^{126}Te(p,3n)^{124}I	36 → 26	190	^{123}I ^{125}I (1.3)	52
	^{123}Te(d,n)^{124}I	11 → 7	2.6	–	52
	^{124}Te(d,2n)^{124}I	15 → 11	20.4	^{125}I (1.2)	52
^{140}Nd	^{141}Pr(p,2n)^{140}Nd	30 → 15	210	–	53
	^{nat}Ce(^{3}He,*x*n)^{140}Nd	35 → 20	12	–	53
			5	–	54
^{165}Er	^{165}Ho(p,n)^{165}Er	16 → 7	79	–	55
	^{165}Ho(d,2n)^{165}Er	20 → 0	300	–	56
^{167}Tm	^{167}Er(p,n)^{167}Tm	15 → 8	6.9	^{166}Tm (0.04)	57
	^{165}Ho(α,2n)^{167}Tm	35 → 20	3.4	^{168}Tm (0.58)	58
^{191}Pt	^{nat}Ir(p,*x*n)^{191}Pt	30 → 15	13	^{189}Pt (500)	59
	^{nat}Ir(d,*x*n)^{191}Pt	19 → 9	11	^{193m}Pt (90)	60
	^{nat}Os(α,*x*n)^{191}Pt	38 → 16	3.6	^{188}Pt (1.5), ^{189}Pt (400), ^{193m}Pt (26)	61, 62
	^{192}Os(^{3}He,4n)^{191}Pt	36 → 25	6.7	–	63
^{193m}Pt	^{192}Os(α,3n)^{193m}Pt	40 → 30	10	^{195m}Pt (0.6)	64
	^{nat}Ir(d,*x*n)^{193}Pt	19 → 9	~ 10	^{191}Pt (> 100)	60
^{195m}Pt	^{192}Os(α,n)^{195m}Pt	24 → 9	0.05	–	64
^{201}Tl	^{203}Tl(p,3n)^{201}Pb → ^{201}Tl	29 → 24	78.5 [e]	^{200}Pb (0.9), ^{202m}Pb (0.05)	37
^{203}Pb	^{nat}Tl(p,*x*n)^{203}Pb	32 → 18	219	^{201}Pb (200) ^{202m}Pb (83)	65
	^{205}Tl(p,3n)^{203}Pb	32 → 18	310	^{202m}Pb (38)	65
	^{nat}Tl(d,*x*n)^{203}Pb	20 → 0	14	^{202m}Pb	66

[a] Hyphen denotes the absence of relevant data in the cited references; [b] a Cu_3As target; [c] yield measured 6.6 h post end of bombardment (EOB); [d] an Al_2Te_3 target; [e] calculated for the maximal ^{201}Tl accumulation time (31.7 h post EOB).

When zinc of natural isotopic composition is irradiated, the by-product ^{66}Ga is generated simultaneously by three routes, the most important being ^{66}Zn(p,n)^{66}Ga and ^{68}Zn(p,3n)^{66}Ga and the least important being ^{67}Zn(p,2n)^{66}Ga. As a result, the plot for cumulative ^{66}Ga generation cross section *versus* energy has two peaks, in the regions of 12 and 35 MeV.[67]

The survey over experimentally determined cross sections and ^{66,67,68}Ga yields in proton-induced reactions on zinc isotopes was published by Szelecsényi *et al.*[38]

Gallium-67 is generated by irradiation of natural zinc with deuterons. The formation of final product is contributed by the reactions ^{66}Zn(d,n)^{67}Ga ($E_{thr} = 0$) (hereafter, E_{thr} stands for the threshold energy), ^{67}Zn(d,2n)^{67}Ga ($E_{thr} = 4.1$ MeV) and ^{68}Zn(d,3n)^{67}Ga ($E_{thr} = 14.6$ MeV). Here (as with proton bombardment, too), the challenge is the generation of ^{66}Ga, which is produced in amounts about one order of magnitude greater than the ^{67}Ga amounts. When a zinc target of natural composition is bombarded by deuterons with an energy of 19 MeV, the ^{67}Ga yield is 16 MBq μA^{-1} h^{-1} and the ^{66}Ga yield is $\sim$140 MBq μA^{-1} h^{-1}. ^{64}Cu ($\sim$31 MBq μA^{-1} h^{-1}) is produced under the same conditions; therefore, two valuable radionuclides can be produced at the same time.[68]

A ^{66}Zn-enriched target can be used for producing small ^{67}Ga amounts; the ^{67}Ga yield in the reaction ^{66}Zn(d,n)^{67}Ga at 11 MeV is 30 MBq μA^{-1} h^{-1}, and ^{66}Ga is not generated in significant amounts.[39]

Ion-exchange chromatography and(or) liquid extraction are usually used to separate gallium from targets. Gallium can be separated from the bulk of a zinc target by extraction with diisopropyl ether from 7 M HCl.[69] Zinc and gallium can be separated on a cation-exchange column in hydrochloric medium. Zinc, unlike gallium, is not retained in 10 M HCl; gallium can then be eluted by 4 M HCl. In this case, copper is eluted together with zinc.[70]

In ammonia media, gallium occurs as $[Ga(OH)_4]^-$ anion and is not retained on a chromatographic column packed with a cation-exchanger, unlike zinc and copper, which yield $[M(NH_3)_4]^{2+}$ ammoniates.[71]

Enriched zinc is regenerated by sorption from 2 M HCl on an anion-exchange column where copper, cobalt and nickel radionuclides are not retained, followed by elution of zinc from the column by water.[69]

III.2. Bromine-77

Bromine-77 is of interest as a therapeutic Auger emitter; its advantages include the ease of incorporation into biomolecules *via* strong chemical bonding to carbon. Bromine-77 can be produced by proton irradiation of selenium. The target should be enriched in ^{78}Se in order to avoid ^{76}Br (16.2 h) impurities. In the energy range 25 → 15 MeV, the main reaction is ^{78}Se(p,2n)^{77}Br ($E_{thr} = 12.81$ MeV); the reaction ^{78}Se(p,3n)^{76}Br needs higher energies to occur ($E_{thr} = 23.97$ MeV).[40]

The reaction ^{77}Se(p,n)^{77}Br ($E_{thr} = 2.18$ MeV) can serve as an alternative production route. In this case, the energy should be confined to $\sim$14 MeV in order to inhibit impurity generation by the reaction ^{77}Se(p,2n)^{76}Br ($E_{thr} = 13.33$ MeV). When there are no very severe requirements as to radioisotope purity, ^{77}Br can also be produced from selenium of natural isotopic composition. Relatively short-lived ^{75}Br (1.6 h) in considerable amounts and ^{76} Br in amounts commensurate to the target product amount are also produced; they can then be used for the PET imaging of distribution of the pharmaceutical in the body.[41]

Pelletized Cu_2Se was also used as a target; radioactive bromine was distilled from the target at $\sim$1100 °C in flowing argon.[72]

The reaction ^{75}As(α,2n)^{77}Br yields almost pure ^{77}Br as arsenic has only one stable isotope and ^{76}Br formation by the (α,3n) route starts at $\sim$28 MeV. A disadvantage of the method consists in a relatively low yield. Challenges can appear in the manufacture of the target, as metallic arsenic does not withstand high thermal and radiation loads and bromine can vaporize during irradiation. A Cu_3As alloy was proposed for use as a target due to its high thermal stability and thermal conductivity.[42] In this case, ^{67}Ga can simultaneously be produced by the reaction ^{65}Cu(α,2n)^{67}Ga.[71] Bromine-77 was distilled from the target at 900 °C in flowing helium; it was condensed on the inner wall of a silica tube whose outer walls were cooled with water; then, bromine was washed with minimal water.

III.3. Technetium-99m

Technetium-99m accounts for 85% of the diagnostic studies in nuclear medicine. This radionuclide has been used for diagnostic purposes during more than half a century, and it is only now that some interest arises in its therapeutic potential. Despite a long history of use, there are yet some challenges in ^{99m}Tc production. Prospects of its production are well documented (see, for example Refs 73 – 75), so here we will consider this issue only in the most general terms.

A classic route to the production of ^{99}Mo, the technetium precursor, is irradiation of ^{235}U in a reactor. This route makes it possible to produce ^{99}Mo with high specific activity, which is required for the production of high-output chromatographic ^{99m}Tc generators. However, disruptions in supply occur periodically because of the narrow circle of the world's manufacturers and the great age of reactors. Further, in accordance with regulatory requirements, high enriched uranium should be withdrawn from the civil circulation and replaced by low enriched uranium (< 20% ^{235}U), which will lead to a fivefold increase in product cost.

Currently, a number of alternative ways to obtain ^{99}Mo are considered, for example, ^{100}Mo(γ,n)^{99} Mo, ^{100}Mo(n,2n)^{99}Mo, ^{98}Mo(n,γ)^{99}Mo and ^{100}Mo(p,pn)^{99}Mo reactions, but all of them fail to provide the specific activity required for the types of generators now in use.

Carrier-free molybdenum-99 can be obtained *via* irradiation of ^{96}Zr with α-particles by the reaction ^{96}Zr(α,n)^{99}Mo. This reaction yields no side products, but its cross section is relatively low ($\sigma_{max} \approx 160$ mbarn at 17 MeV),[44] the ^{96}Zr abundance in the natural mixture is as low as 2.8%, and α-particle beams are relatively difficult to access.

Apart from being released from parent molybdenum, ^{99m}Tc can be generated by irradiating ^{100}Mo by ^{100}Mo(p,2n)^{99m}Tc and ^{100}Mo(p,pn)^{99}Mo → ^{99m}Tc reactions. A drawback of this method is a ^{99g}Tc admixture (250 thousand years), whose formation cross section is about three times as great and the reaction excitation function is slightly shifted toward high energies ($\sigma_{max} \approx 800$ mbarn at 17 MeV) compared to the respective values for ^{99m}Tc ($\sigma_{max} \approx 300$ mbarn at 15 MeV). The longer the irradiation, the higher the ^{99g}Tc percentage. Upon 6-h exposure, the ^{99m}Tc percentage is 21 mass % (18 → 10 MeV) at the end of bombardment (EOB). Gagnon *et al.*[43] showed the feasibility to produce large amounts of ^{99m}Tc, at

a level of terabecquerels, in one session (dose per patient: ~1 GBq). The high target enrichment is of fundamental importance; otherwise, side products can be produced: $^{94m+g}$Tc, $^{95m+g}$Tc, $^{96m+g}$Tc, $^{97m+g}$Tc and other.

The critical analysis of ^{99}Mo/^{99m}Tc production methods published by Wolterbeek *et al.*[76] leads to unpleasant conclusions: in the nearest future, the reactor method will continue to dominate; new types of reactors are needed in order to involve ^{99}Mo with low specific activity into circulation; and the direct production of ^{99m}Tc on cyclotrons is of low promise for the reason of an excess of ^{99g}Tc.

III.4. Indium-111

Indium-111, similarly to ^{99m}Tc, ^{67}Ga and ^{123}I, is among the most popular SPECT radionuclides and, as all of them, is regarded to be a potential therapeutic radionuclide, an Auger electron emitter. It is usually produced *via* proton irradiation of metallic cadmium. For ^{111}In production by the reaction ^{111}Cd(p,n)^{111}In, the optimal energies are in the range up to 15 MeV; when the reaction ^{112}Cd(p,2n)^{111}In is used, the energy range is from 11 to 30 MeV.[37] The yield of the second reaction is far higher. When targets of natural isotopic composition are used, an admixture of relatively long-lived ^{114m}In (49.5 days) is inevitably generated by the reaction ^{114}Cd(p,n)^{114m}In. The irradiation of a thick target by 30-MeV protons produces ~1% ^{114m}In. The generation of other isotopes does not make a challenge in view of their short half-lives.[77]

There are a number of studies into ^{111}In production by deuteron irradiation of cadmium; however, this method is rather of scientific interest because of the low availability of moderate-energy deuteron beams.[78, 79]

The bombardment of a silver target by α-particles yields ^{111}In with an acceptable radioisotopic purity (free of ^{114m}In) but in a lower yield.[45] The optimal energy range is 38 → 15 MeV. ^{111}In was separated from silver by extraction with 15% solution of bis(2-ethylhexyl) phosphoric acid (HDEHP) in hexane from 3.5 M HNO_3.[80] Then, ^{111}In was back-extracted with 50% HBr. Additional purification consisted in the extraction of indium by butyl acetate followed by stripping with water.

For releasing indium from a cadmium target, it was co-precipitated with iron(III) hydroxide by ammonia.[81] Cadmium remained in solution. Then, the precipitate was dissolved in 6 M HBr and then indium, together with iron, was separated from copper and zinc (from the substrate) by extraction with diisopropyl ether. Indium was stripped with 7.7 M HCl, as it does not form stable complexes under those conditions, to leave iron in the organic phase. The aqueous phase was passed through a column packed with Dowex 1 × 8, and then indium was eluted with 0.05 M HCl. This stage provided separation from trace cadmium and a reduction in acidity of ^{111}In-containing solutions.[81]

III.5. Antimony-119

Antimony-119 has very favourable nuclear-physical characteristics,[82] but its therapeutic application is now hindered primarily by the lack of suitable chelating agents. Antimony-119 can be produced by the (p,n) reaction from ^{119}Sn. The reaction ^{119}Sn(p,2n)^{118m}Sb occurs at higher beam energies (E_{thr} = 11.0 MeV). Small amounts of ^{118m}Sb make no serious problem in view of its short half-life (5.0 h). The amount of other impurities, specifically ^{120m}Sb (5.76 days), is determined by the enrichment of the target material.

Ion-exchange chromatography on the low-basicity anion-exchanger Bio-Rad AG4 × 4 in 0.8 M HCl was used to release the desired product from the target. Antimony was the first to leave the column, followed by tin. It is important that both elements should be in their highest oxidation states (V and IV, respectively); for providing this, H_2O_2 was added to concentrated HCl to dissolve the metallic tin target.[47]

III.6. Iodine-123

The major method for preparing this medical radionuclide is to irradiate ^{124}Xe by protons. The desired product is formed through intermediate ^{123}Xe (2.08 h) by two reactions: ^{124}Xe(p,2n)^{123}Cs → ^{123}Xe → ^{123}I and ^{124}Xe(p,pn)^{123}Xe → ^{123}I. The former is of most importance (σ_{max} ≈ 660 mbarn at 25 MeV).[37] The direct generation of ^{123}I as a result of the (p,2p) reaction makes no essential contribution. An advantage of the method is the high purity of the product; other isotopes are not generated under these conditions. Xenon-123 can also be produced by the reaction ^{127}I(p,5n)^{123}Xe, but the reaction cross section peaks in the region of 55 MeV and this considerably limits the range of facilities that can implement the method. One more limitation is the formation of an impurity of long-lived ^{125}I *via* the ^{125}Xe (16.9 h) intermediate by the reaction ^{127}I(p,3n)^{125}Xe → ^{125}I. Iodine is isolated by washing the inner walls of the target vessel.

Since highly enriched ^{124}Xe became available, ^{123}I production from tellurium targets was no longer topical. However, ^{123}I in amounts sufficient for medical applications can be produced by the reaction ^{123}Te(p,n)^{123}I in the range of energies of 18 → 8 MeV (σ_{max} ≈ 580 mbarn at 13 MeV).[37] Interfering reactions do not occur on ^{123}Te under these conditions, so the product purity is determined by the enrichment grade of the target material. The reaction ^{124}Te(p,2n)^{123}I affords a greater amount of the product. ^{124}I formation is unavoidable in principle, but the proper choice of beam energy can help to reduce its amount to less than 1%.[83] The preparation and recycling of tellurium targets will be described in the next section.

III.7. Iodine-124

Iodine-124 is mainly of interest as candidate PET radionuclide, however also having a potential for use as a therapeutic Auger emitter. One route to produce iodine-124 is to irradiate ^{124}Te with deuterons with energies in the range 15 → 6 MeV. A drawback of this method is a relatively high percentage (~2%) of the ^{125}I long-lived impurity. The route ^{124}Te(p,n)^{124}I (σ_{max} ≈ 580 mbarn at 12 MeV) is free of this drawback. It is expedient to limit bombardment energies to 12 MeV in order to decrease the production of the ^{123}I impurity. This route has a desired product yield, which is comparable to that of the (d,2n) reaction, with a far lower ^{125}I percentage (< 0.1%). However, both routes have moderate yields and would hardly be able to meet the growing demand for ^{124}I. Large amounts can be produced[51] by the reactions ^{125}Te(p,2n)^{124}I and ^{126}Te(p,3n)^{124}I. These processes require higher energies of bombarding particles (22 → 15 and 36 → 26 MeV, respectively). The ^{125}I admixture is at a level of 1%.[52] A comparison of the ^{124}I production routes from tellurium has been reported.[52]

Metallic tellurium has no necessary thermal resistance, so glassy tellurium dioxide, added with 6% Al_2O_3 to

improve adherence to the substrate, is more frequently used for preparing targets. Another candidate target material is Al_2Te_3. Such a target withstands currents up to 20 μA.[50] The desired product is separated from the matrix by dry distillation in flowing air at 750 °C (TeO_2) or 910 °C (Al_2Te_3). After this procedure, the target is ready for new bombardment.

Bombardment of antimony with ^{3}He nuclei and α-particles was also considered as routes to prepare ^{124}I. However, these routes are incommensurate to those described above both in output and in product purity.[84]

III.8. Neodymium-140

Neodymium-140 is a promising medical rare-earth radionuclide. The advantages of rare-earth elements include the availability of suitable chelating agents and well-developed methods for incorporating them into biomolecules. However, their production is frequently associated with a difficult task to separate two neighbouring lanthanides, where one lanthanide is, as a rule, in trace amounts and the other is in weight amounts.

Neodymium-140 has attracted particular attention, because not only is it an Auger emitter, but also an *in vivo* generator of ^{140}Pr, a short-lived (3.4 min) positron emitter which is also a source of Auger electrons. Neodymium-140 can be produced by the reaction ^{141}Pr(p,2n)^{140}Nd, which does not yield long-lived isotope impurities. The merit of this production route consists in that natural praseodymium contains one stable isotope. The reaction has $\sigma_{max} \approx 900$ mbarn at 18 MeV; the optimal energy value for the production is $25 \rightarrow 15$ MeV.[53]

The reaction ^{nat}Ce(^{3}He,*x*n)^{140}Nd, which likewise does not yield long-lived impurities, can serve as another preparation route. This route has low yields and ^{3}He beams are not so easily available, but still it has a serious merit in that the separation of Nd and Ce is not so difficult since cerium can be oxidized to the tetravalent state.[54]

III.9. Erbium-165

Erbium-165 is an almost ideal radionuclide for Auger therapy. It has no γ-lines and decays exclusively by the electron capture type. Its half-life approaches the optimal value (10.36 h). Further, it can easily be produced by the reaction ^{165}Ho(p,n)^{165}Er from holmium, which is naturally abundant as the only isotope with mass number 165. The excitation peak of this reaction is in the range 9 – 10 MeV, $\sigma_{max} \approx 170$ mbarn. The cyclotron yield for a maximal beam energy of 11 MeV is 41 MBq μA^{-1} h^{-1}, and for 15 MeV, it is 75 MBq μA^{-1} h^{-1}. The use of a 30-MeV beam makes it possible to double the yield (142 MBq μA^{-1} h^{-1}), but when the peak energy exceeds 17 MeV, the (p,3n) reaction proceeds to yield relatively short-lived ^{163}Er (1.25 h).[55] Since erbium isotopes with mass numbers of 162 and 164 are stable, other radioisotope impurities are not formed.

The reaction ^{165}Ho(d,2n)^{165}Er has $\sigma_{max} \approx 600$ mbarn at 12 – 14 MeV and a far higher product yield compared to that of the (p,n) reaction.[56] The feasibility to prepare ^{165}Er free of a considerable admixture of the target material was shown. For this purpose, a holmium (~15 mg) and erbium mixture was sorbed on a column (4×120 mm^2) packed with the Aminex A5 (Bio-Rad) cation-exchange resin and then eluted with 0.15 M α-HIBA at pH 5 (HIBA stands for α-hydroxyisobutyric acid). Separation was achieved in two stages; the column used for final refinement had a smaller capacity.[85]

III.10. Thulium-167

Thulium-167 has long been regarded as a promising therapeutic radionuclide, but its production has certain challenges. Natural erbium consists of six stable isotopes, so proton bombardment yields a mixture of radioactive thulium isotopes, most of them being relatively long-lived. The only acceptable variant is the reaction ^{167}Er(p,n)^{167}Tm ($\sigma_{max} \approx 400$ mbarn at 10 – 11 MeV). The production of side product ^{166}Tm (7.7 h) by the (p,2n) reaction starts at about 10.5 MeV, but this makes no problem as it has a short half-life. In contrast, ^{168}Tm (93.1 days) formation by the ^{168}Er(p,n)^{168}Tm reaction is very undesirable, making important a high enrichment of the target. When enrichment was 95.6%, the ^{168}Tm percentage on day 5 post EOB was 0.2%.[57]

Several indirect methods were proposed for preparing ^{167}Tm,[86] but they all require a rapid and efficient separation of neighbouring lanthanides. The most interesting route is ^{168}Yb(p,2n)^{167}Lu → ^{167}Yb → ^{167}Tm, which can be implemented with good yield on a moderate-energy cyclotron (< 30 – 35 MeV). The cross section of this reaction, equal to 1300 mbarn at 24 MeV, is three times that for the ^{167}Er(p,n)^{167}Tm reaction, but the abundance of ^{168}Yb in the natural mixture is as low as 0.13%.

Deuteron and α-particle reactions have far lower yields than proton reactions. The ^{166}Er(d,n)^{167}Tm route can be used, but the σ_{max} of the reaction is as low as 23 mbarn at 10 MeV.[87] The ^{167}Er(d,2n)^{167}Tm reaction has a far higher yield, but the product is contaminated with long-lived ^{168}Tm produced in the concurrent (d,n) reaction.

The merit of the ^{165}Ho(α,2n)^{167}Tm reaction is the use of a natural holmium target (it consists of the only isotope with mass number 165). However, in this case, too, long-lived ^{168}Tm is inevitably formed through the (α,n) route. The selection of an optimal energy range can help to reduce ^{168}Tm percentage to 0.32% (with a beam energy of $35 \rightarrow 25$ MeV).[58]

III.11. Platinum-191, 193m and 195m

Platinum has a number of isotopes that are promising for Auger therapy, but the production of unsupported radioactive platinum meets certain challenges, as will be shown below. The precursor material can be osmium or iridium.

The cross sections of reactions induced by α-particles on ^{192}Os were studied in the range of energies from 16 to 40 MeV. The ^{192}Os(α,n)^{195m}Pt reaction has a very low cross section (~ 2 – 4 mbarn as reported in Ref. 88 and ~ 5 – 10 mbarn as reported in Ref. 64) and thereby is unsuitable for the production of therapeutic ^{195m}Pt doses. Small ^{195m}Pt amounts can be produced in the range $24 \rightarrow 9$ MeV, where no side processes occur and the product purity is determined by the degree of enrichment of the target material.

The increasing energies of bombarding particles initiate the ^{192}Os(α,3n)^{193m}Pt process [the reaction energy (Q) is −23.19 MeV], which has a high cross section ($\sigma_{max} \approx$ 1500 mbarn at 36 MeV). The energy range $40 \rightarrow 30$ MeV is reported to be optimal for ^{193m} Pt production.[64] Only a small impurity of ^{195m}Pt is generated under these conditions, which makes no problem because of a similarity of the nuclear-physical properties of ^{193m}Pt and ^{195m}Pt.

The ^{3}He bombardment of ^{192}Os can serve to produce ^{191}Pt of high radioisotope purity.[63] Experiments showed that ^{193m}Pt was not formed.[88] Product yields are moderate, but up to 500 MBq can be produced per session. Another possible route to prepare ^{191}Pt is the bombardment of a natural osmium target with α-particles, but yields are also moderate and impurity contents are high.[61]

Osmium targets were prepared by electrowinning from an alkaline solution of potassium perosmate on a nickel substrate. After being bombarded, the target together with the substrate was dissolved in 2 ml of conc. nitric acid and the solution was heated until complete evaporation. The osmium was trapped as tetroxide by 4.7 M KOH. The dry residue comprised nickel from the substrate and radioactive platinum. The residue was dissolved in 5 ml of 3 M HCl, and 0.5 ml of freshly prepared 10% $SnCl_2$ solution in 3 M HCl was added. The platinum was thus reduced to the divalent state and then could be quantitatively extracted by diethyl ether {extractable species: $[Pt(SnCl_3)_5]^{3-}$}.[64]

Tárkányi *et al.*[59] studied proton-induced reactions on natural isotopic iridium. However, they failed to measure the ^{193m}Pt yield because of the low cross section of formation of this nuclide and difficulties of its spectrometric determination. The authors only reported the value of 100 mbarn calculated for the cross section of ^{193}Ir(p,n)$^{193m+g}$Pt reaction for 12 MeV. Finally, they rejected this method as inefficient for preparing ^{193m}Pt. However, the method can be applied to prepare ^{191}Pt; in this case, the major reaction will be ^{193}Ir(p,3n)^{191}Pt and the ^{191}Ir(p,n)^{191}Pt process will make a much lower contribution. The maximal cross section of the ^{nat}Ir(p,*x*n)^{191}Pt process is ~600 mbarn at 30 MeV; a considerable amount of ^{189}Pt (10.87 h) is produced simultaneously. Optimal energies for producing ^{191}Pt should not exceed 30 MeV; the relatively long-lived ^{188}Pt (10.2 days) is not formed.[59]

The deuteron bombardment of iridium targets in the energy range 20 → 10 MeV yields a mixture of platinum isotopes ^{191}Pt and ^{193m}Pt in close proportions[60] as a result of (d,2n) reactions on ^{191}Ir and ^{193}Ir, respectively. At higher deuteron energies, ^{188}Pt and ^{189}Pt are also generated.

We failed to find documents concerning reactions on stable iridium isotopes. A comparison of ^{191}Pt production methods can be found by Qaim *at al.*[63]

There are indications that ^{195m}Pt was prepared by a photonuclear route by bombarding gold with bremsstrahlung photons with energies up to 34 MeV by the reaction ^{197}Au(γ,np)^{195m}Pt,[89] but the yields were not reported. The specific activity of the desired product was slightly reduced due to the simultaneous generation of the stable platinum isotope by the reaction ^{197}Au(γ,n)^{196}Au → ^{196}Pt.

III.12. Thallium-201

Thallium-201 is widely used for SPECT, but it also has a therapeutic potential. The only today's method to produce thallium is an indirect route through ^{201}Pb (9.33 h), which is produced by bombarding ^{203}Tl by the reaction (p,3n). A challenge can arise from (p,2n) and (p,4n) processes, which yield ^{202m}Pb (3.53 h) and ^{200}Pb (21.5 h). The former decays to ^{202}Tl (12.23 days) with 9.5% probability and the latter exclusively to ^{200}Tl (1.09 days).

The (p,2n) reaction on ^{203}Tl has a maximal cross section at 21 – 22 MeV, the (p,3n) reaction has at 28 MeV and the (p,3n) reaction at ~40 MeV. In other words, the range of optimal bombardment energies is very narrow, and its choice is dictated by a compromise between the amount of the product and its purity. Nuclear data for proton-induced reactions on ^{203}Tl are summarized in Ref. 90, the survey over reactions on natural thallium is found in Ref. 91.

Thallium can be freed from lead traces by co-precipitation with $Fe(OH)_3$ or by ion-exchange chromatography in 0.025 M EDTA at pH 4 on a column packed with Dowex 50 × 8 (thallium is sorbed, whereas lead passes through the column).[92] Trace amounts of lead and thallium can be separated in 3 M HCl on Dowex 1 anion-exchanger: thallium(I) passes through the column far more rapidly than lead does.[93]

III.13. Lead-203

When thallium of natural isotopic composition is irradiated, ^{203}Pb is generated by two reactions: ^{203}Tl(p,n)^{203}Pb and ^{205}Tl(p,3n)^{203}Pb. The former of these reactions, however, has a low cross section and can hardly be used in practice. The product yield increases rapidly as the beam energy increases, due to the reaction ^{205}Tl(p,3n)^{203}Pb, but ^{201}Pb (9.33 h) is concurrently generated in considerable amounts by the reaction ^{203}Tl(p,3n)^{201}Pb. This challenge is avoidable if a ^{205}Tl target is used. The published excitation functions[94] imply that the optimal range of energies is 32 → 18 MeV.

Deuteron-induced reactions on thallium can serve to prepare ^{203}Pb. The excitation function of the ^{nat}Tl(d,*x*n)^{203}Pb reaction has two peaks; the peak (σ_{max} = 170 mbarn) at ~15 MeV corresponds to the ^{203}Tl(d,2n)^{203}Pb process, and the peak (σ_{max} = 800 mbarn) at 29 – 33 MeV corresponds to ^{205}Tl(d,4n)^{203}Pb. In this case, there is no need to use an enriched target: the reaction ^{203}Tl(d,4n)^{201}Pb, which yields a side product, has a threshold of 19.8 MeV, so a relatively short-lived ^{202m}Pb (3.53 h) is the only impurity at 20 MeV. The yield of desired product under these conditions is not very high; it rises as the particle energy increases, but with a decline in radioisotope purity.[66, 95]

Lead-203 can also be produced by the bombardment of mercury with α-particles or ^{3}He nuclei, for example, by the reaction ^{201}Hg(α,2n)^{203}Pb or ^{202}Hg(^{3}He,2n)^{203} Pb, but we failed to find relevant experimental data in the literature. The results of modelling have been reported.[96]

IV. Characteristics of α-emitters that show a potential for medical applications

β-Emitting radionuclides are now the key therapeutic radionuclides due to their availability and well-developed technology to load them onto vehicles, which are usually antibodies.[22] However, α-emitters are attracting the increasing attention due to advances in their production technologies and loading onto vehicles (Table 6).

Indeed, there are a number of properties that make α-emitters more preferable than β-emitters (for a certain range of applications). For example, α-particles have LETs in the range 50 – 230 keV μm^{-1}, which is two orders of magnitude higher than for β-particles (0.1 – 1.0 keV μm^{-1}). The ranges of α-particles are several cell diameters against ranges of up to one centimetre for β-particles.[22] The relative biological effectiveness (RBE), which is determined as the absorbed dose ratio of the tested radiation to the reference radiation that causes the same effect (γ -radiation of ^{60}Co), for α-particles is 3 – 8 against unity for β-radiation.[97] Due to

Table 6. Characteristics of selected α-emitters of medical importance.[3, 22]

Radionuclide	α-Particle energy /MeV	Half-life	Range /μm
^{225}Ac	5.8 – 8.4	9.92 days	50 – 90
^{211}At	5.9/7.5	7.2 h	55 – 80
^{212}Bi	6.1/7.8	60.6 min	40 – 100
^{212}Pb	6.1/7.8	10.6 h	40 – 100
^{213}Bi	5.9/8.4	45.6 min	50 – 90
^{223}Ra	5.7 – 7.4	11.4 days	50 – 70
^{149}Tb	4.0	4.1 h	30

this, the cytotoxicities of α-emitters are 5 – 100 times those of β-emitters.[98] α-Particles cause complex double-strand breaks in DNA, which are poorly repairable by cells.[99] For example, the yield of double-strand DNA breaks caused by exposure to ^{211}At-emitted α-particles was ~10 breaks per billion of DNA base pairs and per Gray,[100] which is 25 – 75 times greater than for Auger emitters (see Table 1). The cellular nucleus, more exactly, the nuclear DNA, is the most sensitive target to the effect of α-particles, and its damage leads to the death of the cell.[30] One more important feature of the cytotoxic effect of α-emitters consists of the following: they show no weakening of radiation damage under hypoxia/anoxia [101] unlike sparsely ionizing radiation, which is important for the therapy of tumours where the oxygen content is reduced. The expedience to deliver α-emitters into target cellular nuclei is obvious from the consideration of *S* values (Table 7).

The utility of ^{225}Ac is limited by its relatively long half-life and by the occurrence of three daughter α-emitters in the chain, which leave the parent radiopharmaceutical molecule due to the recoil effect and can, under certain conditions, be redistributed over the body to give rise to undesirable side effects. The challenges associated with the recoil effect are also typical of the ^{212}Pb/^{212}Bi *in vivo* generator. Although the recoil energy upon β-decay is not high (~0.5 eV), the ^{212}Bi daughter nucleus undergoes internal conversion in more than 40% of cases to destroy chemical bonds and release ^{212}Bi. One way to avoid undesired consequences of the recoil effect is to use vehicles that rapidly penetrate into cells.

The cytotoxicity of ^{213}Bi-DTPA-F3 and ^{225}Ac-DTPA-F3 peptide agents, where the peptide F3 linked to a diethylenetriaminepentaacetic acid (DTPA) moiety provides for the delivery of the radionuclide into cancer cell nuclei, was tested *in vitro* for colony-forming ability.[102] The ID_{50} (half-inhibition dose) values for ^{213}Bi-DTPA-F3 and ^{225}Ac-DOTA-F3 were 53 and 67 Bq ml^{-1}, respectively. Therapeutic studies on two sets of laboratory mice with xenotransplanted cancer cells showed that the use of six doses, each of 1.85 kBq ^{225}Ac-DOTA-F3 and 1.85 MBq ^{213}Bi-DTPA-F3, caused an increase in animal survival time up to 95 and 97 days, respectively; that is, the ^{225}Ac activity required for attaining the same effect was three orders of magnitude lower than the ^{213}Bi activity. Importantly, the effect of RPs comprising short-lived ^{213}Bi causes a rapid shrinkage of the tumour in 30 days, whereas RPs comprising the longer-lived ^{225}Ac cause a similar tumour shrinkage in a longer period.

Table 7. Dose absorbed per unit total radioactivity for selected α-emitters.[34]

Radionuclide	S /Gy Bq^{-1} s^{-1}		S(N ← N) : S(N ← CS)
	N ← N	N ← CS	
^{212}Bi	2.82×10^{-2}	5.50×10^{-3}	5.1
^{210}Po	8.19×10^{-2}	1.62×10^{-2}	5.1

V. Production of medical α-emitters

V.1. Terbium-149

Terbium-149 has a unique combination of nuclear-physical and chemical properties; it is the only short-lived α-emitter among the lanthanides. Unlike ^{223}Ra, terbium-149 can be firmly bound to biomolecules; its half-life is better suitable for therapeutic purposes than that of ^{213}Bi. Recent studies [103] showed the anticancer activity of ^{149}Tb-containing pharmaceuticals. Unfortunately, there are no facile pathways to produce this radionuclide. In those studies, ^{149}Tb was produced by spallation from a hot bulk tantalum target followed by the online separation of products (at the ISOLDE facility at CERN). The radiochemistry of release consisted of the cation-exchange separation of ^{149}Tb and ^{149}Gd isobars (elution with 0.13 M α-HIBA) and some other lanthanides. In this way, 25 MBq ^{149}Tb was produced per session.

The reaction ^{152}Gd(p,4n)^{149}Tb ($Q = -28.21$ MeV) has a very high yield (~2500 MBq μA^{-1} h^{-1} in the range 66 → 30 MeV);[104] however, its application is hampered by the low natural abundance of ^{152}Gd (0.2%) and by numerous side reactions.

V.2. Astatine-211

Astatine-211 is among the most promising α-emitters due to its optimal half-life and the similarity to iodine. However, it has a limited application, primarily because of production challenges.[105] The only route to produce astatine-211 is the reaction ^{209}Bi(α,2n)^{211}At, which has $E_{thr} = 20.72$ MeV and $\sigma_{max} \approx 950$ mbarn at 31 MeV.[106] However, the beam energy should not exceed the threshold of the reaction ^{209}Bi(α,3n)^{210}At, which is 28.61 MeV, as an even minor ^{210}At (8.1 h) impurity is hazardous for it decays to yield highly toxic ^{210}Po. The experimentally determined ^{211}At yield is 38 MBq μA^{-1} h^{-1} at 29.5 MeV (Ref. 107) (the ^{210}At percentage under these conditions is less than 0.1%) and 32 MBq μA^{-1} h^{-1} at 29 MeV.[106] Polonium-210 can be produced not only from ^{210}At, but also by the direct route ^{209}Bi(α,p2n)^{210}Po ($E_{thr} = 23.31$ MeV).

The most popular method to release astatine from a bismuth target is dry distillation in flowing air, nitrogen or argon at 650 – 670 °C. Polonium is not volatile under these conditions.[108] A possible alternative is the extraction of astatine by diisopropyl ether.[109, 110]

V.3. Actinium-225 and bismuth-213

Actinium-225 is one of the most promising α-emitting radionuclides, which can be used both directly [18, 102, 111] and to produce daughter ^{213}Bi (46 min) in isotope generators. The major ^{225}Ac production method is to release it from ^{233}U fission products:[112 – 114] ^{229}Th (7340 years) → ^{225}Ra (14.8 days) → ^{225}Ac. Thorium-229 is isolated from ^{233}U stocks of nuclear weapons programmes. The main limitations of this method are the

Table 8. Estimates of the worldwide ^{225}Ac production from ^{229}Th.[115]

Production facility	Physics and Power Engineering Institute, Obninsk, Russia	Oak Ridge National Laboratory, Oak Ridge, USA	Institute for Transuranium Elements, Karlsruhe, Germany
^{229}Th /GBq	5.55	5.55	1.7
Maximal annual production of ^{225}Ac /GBq	26.6	22.2	13

relatively low availability of the 'old' ^{233}U, which had enough time to pile up at least insignificant amounts of daughter ^{229}Th and, accordingly, ^{225}Ac. The annual world production of ^{225} Ac from ^{229}Th is ~61.8 GBq (Table 8) [115] with the potential worldwide demand estimated at >1.85 TBq year^{-1}.

The designs of ^{229}Th/^{225}Ac isotope generators are discussed in detail in Guseva's survey.[116] Generator systems are described where parent ^{229}Th is sorbed on titanium phosphate,[117] from which ^{225}Ac can periodically be eluted. In another version, parent ^{229}Th is in a 0.25 M ammonium citrate solution, from which ^{225}Ac can be released by ion exchange.[118]

The ^{229}Th isotope, from which ^{225}Ac is derived, can also be obtained from ^{230}Th (75 400 years) irradiated by rapid neutrons or γ-quanta.[119] The parent ^{230}Th is a member of the uranium-238 radioactive row; its abundance is ~20 g per tonne of uranium, which makes this material hardly accessible and the method hardly suitable for large-scale production of ^{225}Ac.

Bombardment of ^{226}Ra targets by protons, neutrons or γ-quanta can be used to produce ^{225}Ac.[120–122] However, these methods have not come into wide use in large-scale production of ^{225}Ac because of the need for recycling highly active radium targets. Melville and Allen [123] published a comprehensive discussion of the feasibility to produce large amounts of ^{225}Ra, which is the parent radionuclide for ^{225}Ac, or directly ^{225}Ac through ^{226}Ra irradiation on cyclotrons or linear accelerators. The photonuclear reaction ^{226}Ra(γ,n)^{225}Ra, whose cross section reaches 532 mbarn with photon energy of 13.75 MeV, can be used.[124, 125]

The possibility was shown to produce ^{225}Ac from $^{226}RaCl_2$ targets irradiated on a cyclotron by the reaction ^{226}Ra(p,2n)^{225}Ac. Apostolidis *et al.*[120] varied the proton energy from 8.8 to24.8 MeV; the highest ^{225}Ac yield was achieved when the proton energy was 16.8 MeV (Fig. 1). The ^{226}Ac (29 h) and ^{224}Ac (2.9 h) production was insignificant and did not affect the ^{225}Ac isotopic purity. The irradiation of 30 mg of ^{226}Ra with 16 MeV protons for 45 h can produce ~13 mCi of ^{225}Ac.

The ^{225}Ac was isolated from irradiated radium and radium fission products with two consecutive extraction-chromatographic columns packed with HDEHP (Ln Resin, Eichrom) and 4,4′(5′)-di-*tret*-butylcyclohexano-18-crown-6 (Sr Resin, Eichrom). The first column served to separate radium from dilute hydrochloric acid solutions (0.01 – 0.1 mol litre^{-1}), whereas actinium was eluted by 2 M HCl. The final purification of the actinium from radium fission products was in the second column.

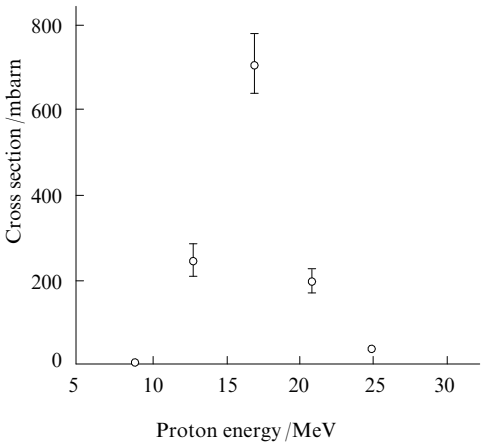


Figure 1. Experimentally determined cross section of the reaction ^{226}Ra(p,2n)^{225}Ac.[120]

A promising method for producing ^{225}Ac in large amounts involves the irradiation of natural ^{232}Th by moderate- and high-energy protons.[126–129] Actinium-225 production by proton bombardment of thorium involves several main reactions: nuclear reaction ^{232}Th(p,p7n)^{225}Th (followed by 10% β^+ decay to ^{225}Ac) and direct reaction ^{232}Th(p,2p6n)^{225}Ac. Figure 2 shows an overall ^{225}Ac yield *versus* proton energy plot. The plot implies that the method is suitable for the production of ^{225}Ac in large amounts, of ~96 GBq (2.6 Ki), by irradiation with 140 MeV protons for 10 days (100 μA beam current).[127] Thus, the method can become the major one for the large-scale production of ^{225}Ac. The main drawbacks of the method are, firstly, the simultaneous formation of long-lived ^{227}Ac (21.8 years), which cannot be separated chemically, and secondly, a limited number of accelerators in the world with proton energies exceeding 100 MeV and with high currents acceptable for producing large amounts of radionuclides. Actinium-227 is generated by reactions ^{232}Th(p,2p4n)^{227}Ac and ^{232}Th(p,α 2n)^{227}Ac, and its impurity accounts for 0.23% of the ^{225}Ac radioactivity (for the above-specified irradiation conditions).[127] The ^{225}Ac yield and ^{227}Ac impurity percent-

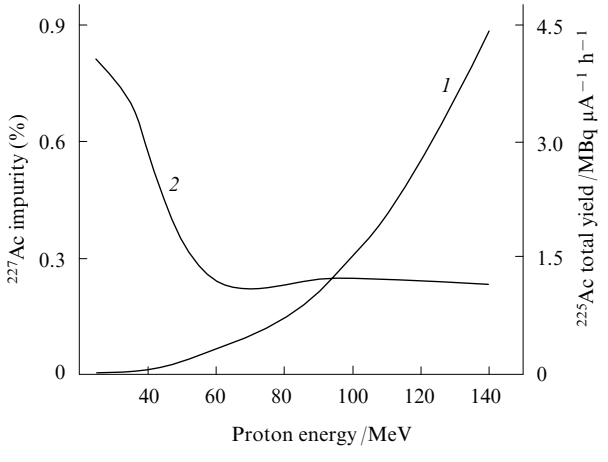


Figure 2. Yield *vs.* proton energy curves for ^{225}Ac (*1*) and ^{227}Ac impurity (*2*).[127]

age are plotted *versus* proton energy in Fig. 2, which implies that a proton energy of $\geqslant$100 MeV is necessary for producing ^{225}Ac in large amounts. However, the ^{227}Ac impurity does not interfere with the use of ^{225}Ac in a ^{213}Bi isotope generator.

The exposure of thorium to moderate- and high-energy protons yields spallation and fission products, specifically ^{224}Ra (3.7 days), ^{225}Ra (14.8 days), ^{226}Ac (29 h), ^{227}Ac (21.8 years), ^{227}Th (18.7 days), ^{228}Th (1.9 years), ^{231}Th (25.5 h), ^{228}Pa (22 h), ^{229}Pa (1.4 days), ^{230}Pa (17.4 days), ^{232}Pa (1.3 days), ^{233}Pa (27 days), ^{230}U (20.8 days), ^{111}Ag (7.5 days), ^{103}Ru (39.3 days), ^{106}Ru (372 days), ^{131}I (8.0 days), ^{126}Sb (12.4 days), ^{127}Sb (3.9 days), ^{125}Sn (9.6 days), ^{123}Sn (129 days), ^{124}Sb (60.3 days), ^{127}Xe (36.4 days), ^{115m}Cd (44.6 days), ^{129m}Te (33.6 days), ^{136}Cs (13.2 days), ^{95}Zr (64.0 days), ^{95}Nb (35.0 days), ^{93}Y (10 h), ^{140}Ba (12.8 days), ^{99}Mo (66 h), ^{141}Ce (32.5 days), ^{148m}Pm (41.3 days), ^{147}Nd (11.0 days) and others (several hundred peaks in γ-spectra).[127, 130] The isolation of ^{225}Ac, whose radioactivity is as low as $\sim$1% of total radioactivity, is a nontrivial analytical problem, which can be solved using a tandem of liquid extraction and extraction chromatography. Aliev *et al.*,[131] after dissolving an irradiated thorium target in HNO_3 with catalytic amounts of HF, carried out liquid extraction with HDEHP two times to separate macro amounts of thorium and some other radionuclides, followed by extraction-chromatographic separation on two consecutive columns packed with sorbents containing *N*,*N*,*N*′,*N*′-tetraoctyl diglycol amide (DGA Resin, TrisKem Int.) and *N*,*N*-diisobutylcarbamoylmethyl(octyl)-phenylphosphine oxide (CMPO), dissolved in tributyl phosphate (TBP) (TRU Resin, TrisKem Int.). The first column provided the group separation of actinium and rare-earth elements, and a radiochemically pure ^{225}Ac fraction was separated on the second column. This separation method was tested on an irradiated bulk thorium target, with chemical yields higher than 85%.

V.4. ^{213}Bi isotope generators

Designs of ^{225}Ac/^{213}Bi isotope generators are described in several papers.[132 – 134] The major distinctions can be reduced to the selection of sorbents and elution media. Guseva and Dogadkin[133, 134] proposed a system of two anion-exchange resins and one cation-exchange resin for a ^{229}Th/^{225}Ac/^{213}Bi triple generator. The first anion-exchange column served for periodical ^{225}Ac elution from thorium with 8 M HNO_3, and the second one served for ^{225}Ac purification from ^{225}Ra and other impurities in HNO_3 – MeOH. The ^{225}Ac was eluted from the second anion-exchange column with 0.1 – 0.2 M HNO_3 and directly supplied to the cation-exchange column to isolate ^{213}Bi, that column being in fact a ^{225}Ac/^{213}Bi isotope generator. Dilute HCl, HBr or DTPA solutions can be used to elute ^{213}Bi.

There are documents describing generator systems designed to use extraction-chromatographic and ion-exchange resins, where sorbents based on Aliquat-336 and Dipex,[135] bis(2-ethylhexyl)methanediphosphonic acid[136] or cation-exchangers were used.[112, 132, 137 – 139] For details of ^{225}Ac/^{213}Bi generators, see Guseva's survey.[116]

V.5. Bismuth-212

Bismuth-212 (60.5 min) has not yet been used for targeted delivery, but a potential of an isotope generator with parent ^{212}Pb (10.6 h) for *in vivo* use was mentioned.[140, 141] A ^{212}Pb/^{212}Bi generator is separated from parent ^{228}Ra (5.7 years), which is in turn separated from 'old' ^{232}Th. For this purpose, thorium is precipitated as hydroxide, and the radium that has remained in solution is further purified on an anion-exchange column in 8 M HNO_3 and exposed to pile-up ^{228}Th.[142, 143] The main limitation imposed on the use of ^{212}Bi arises from its hard γ-radiation (E_γ = 2.6 MeV).

V.6. Radium-223

Of the α-emitting radionuclides, radium-223 (11.4 days) has found clinical use in the form of $^{223}RaCl_2$ solutions having an activity of 1000 kBq ml^{-1}. The pharmaceutical is used for the treatment of metastatic bone cancer, and its activity arises from the similarity of its chemical properties and behaviour to those of calcium (the ability to accumulate in bones). Radium-223 is produced from ^{227}Ac (21.8 years) through an intermediate radionuclide ^{227}Th (18.7 days). Although ^{227}Ac is a member of the ^{235}U row, a more suitable route to obtain it is to irradiate ^{226}Ra with neutrons by the reaction ^{226}Ra(n,γ)^{227} Ra (42.2 min) $\rightarrow$ ^{227}Ac. The thermal neutron capture cross section is $\sim$13 barn.[144] Apart from $RaCl_2$, there is mentioned the usefulness of monoclonal antibodies and liposomes for the targeted delivery of ^{223}Ra to cancer cells.[145, 146]

VI. Production facilities

The IAEA reported[147] that, in 2006, $\sim$350 cyclotrons were used to produce radionuclides over the world. Most of these cyclotrons ($\sim$60%) accelerate protons to 10 – 20 MeV. This is usually sufficient to produce the radionuclides of interest by (p,n) reactions in small quantities. Most widely used ^{67}Ga, ^{111}In, ^{123} I, as well as ^{77}Br, ^{119}Sb, ^{124}I, ^{165}Er and ^{167}Tm can be produced in this way. The advantage of (p,n) reactions is the high isotopic purity of the product; their drawback consists in relatively low yields.

The (p,2n) and (or) (p,3n) reactions, which have, as a rule, high yields, are suitable for the large-scale production of ^{67}Ga, ^{111}In, ^{123}I, ^{124}I and ^{77}Br and for the production of ^{201}Tl, ^{203}Pb, ^{140}Nd and ^{191}Pt. Cyclotrons with proton energies of 20 – 35 MeV are required for this purpose. The drawback of these processes consists in the occurrence of competing reaction paths and, thereby, in lower radioisotopic purity.

Deuteron-induced reactions can serve as an alternative to proton beams, as (d,2n) reactions frequently have higher yields compared with (p,n) reactions, yielding the same products. Deuteron beams are, however, far less available.

Reactions induced by α-particles have very low cross sections compared with proton-induced processes and are applicable only in special cases, for example, to produce ^{211}At, ^{193m}Pt, ^{195m}Pt and, possibly, ^{167}Tm. There are $\sim$40 such accelerators over the world; two of them are in Russia, one in the Kurchatov Institute and the other in Tomsk Polytechnic University.[105]

There are five medium-energy proton accelerators suitable for producing ^{225}Ac/^{213}Bi in the world, one being in the Institute for Nuclear Research of the Russian Academy of Sciences (Troitsk, Moscow).

The use of electron accelerators for the production of medical radionuclides is today hampered by a small number of plants and the lack of nuclear data.

VII. Main families of delivery vehicles for radionuclides that emit short-range particles

Antibodies against specific surface determinants of target cells were historically the first, and still remain the major, radionuclide delivery vehicles for both diagnostic and therapeutic purposes. Even a specific field of radiology emerged with its own tasks, namely radioimmunotherapy, whose main tool was antibodies loaded with radionuclides attached to them.[148, 149] Advances in this field have been due to the advent of radiopharmaceuticals, which are allowed for wide use as written above in the Introduction. However, one should keep in mind that, especially at early times, the produced antibodies were against the determinants (epitopes) that were constantly located on the surfaces of target cells. It was only recently that antibodies were produced against the determinants that experience various endocytosis variants and thereby appear inside target cells together with transported compounds (if were loaded with them). Importantly, internalizable (*i.e.*, penetrating into a cell) vehicles can provide not only for a more pronounced cytotoxicity of the delivered radionuclide, but also for a more optimal biodistribution of the radionuclide. For example, ^{64}Cu-labelled internalizable (cBR96) and non-internalizable (cT84.66) antibodies against colon carcinoma cell antigens differently accumulated in non-target tissues: in the liver, the uptake of ^{64}Cu-DOTA-cT84.66 in 18 h amounted to 17.1% of the administered dose per gram, whereas for ^{64}Cu-DOTA-cBR96, the respective value was as low as 6.55%; in the spleen, the uptake values were 27.4 and 5.19%, respectively. In addition, the uptake rates of internalizable antibodies cBR96 in the tumour were far higher than for uninternalizable cT84.66.[150] This developing line of design and production of antibodies [151] has yet to take its rightful place, specifically in radioimmunotherapy.[7]

As mentioned above, radionuclides emitting short-range particles need to be delivered into the cellular nucleus in the immediate proximity of DNA to express their cytotoxicity (Auger emitters) or to enhance it (α-emitters) and to make a poorly repairable or unrepairable damage to the DNA.

Since the location inside the nuclei of target cells is less important for α-emitters than for Auger emitters (see Tables 3 and 7), delivery vehicles for α-emitters are developed both to deliver them to the surface of a target cell (for example, antibodies against surface epitopes) and to the cell interior. Delivery vehicles for Auger emitters are directed to fulfil only the latter task, namely the delivery to the cell interior and finally into the cellular nucleus.

As regards α-emitters, phase 1–2 clinical trials have been performed with the following radionuclide vehicles:[23, 151 – 154]

1) humanized anti-CD33 antibodies HuM195, carrying ^{213}Bi or ^{225}Ac, for the treatment of acute myeloid leukaemia;

2) monoclonal antibodies 9.2.27 against melanoma-associated chondroitin sulfate proteoglycan (MCSP) carrying ^{213}Bi, for the treatment of metastatic melanoma and glioblastoma;

3) chimeric anti-tenascin monoclonal antibodies loaded with 81C6 ^{211}At and ^{213}Bi-DOTA-[Thi^{8},Met(O$_2$)^{11}]-peptide P for the treatment of glioblastoma;

4) anti-CD20 monoclonal antibodies labelled with ^{213}Bi, for the treatment of non-Hodgkin's lymphoma;

5) F(ab′)$_2$ fragments of the monoclonal antibody MX35 against protein 2b, labelled with ^{211}At, for the treatment of ovarian cancer; and

6) monoclonal anti-HER2/neu antibodies Trastuzumab® (Herceptin) that carry ^{212}Pb, for the treatment of ovarian cancer.

In this listing, only substance P derivative (an 11-membered oligopeptide, type 1 neurokinin receptor ligand) is not an antibody or an antibody fragment while the other α-emitter vehicles used in the above-listed clinical studies are. In our opinion, this signifies that, in the nearest future, we should expect a splash of interest in the intracellular (intranuclear) delivery of α-emitters (see below). Pioneering works have already been published where the authors showed a considerable increase in efficacy of α-emitters upon their intracellular and, especially, intranuclear delivery.[155, 156] Boudousq *et al.*[155] compared the anti-tumour activities of a ^{212}Pb α-emitter when it was delivered to epidermoid human carcinoma A431 by antibodies against the non-internalizable CEA antigen (cancer embryonic antigen) and by antibodies against internalizable HER2. The efficacy of the ^{212}Pb delivered to cells by the antibodies against the internalizable antigen when calculated per Gray appeared to be higher than for the ^{212}Pb delivered by the anti-CEA antibodies. The study by Rosenkranz *et al.*[156] will be discussed below in the context of modular nanotransporters.

Almost the first attempts to use Auger electron emitters in medical practice rather than for research purposes showed the need to develop such vehicles that would not only recognize target cells but also penetrate them and, moreover, move into the cell nucleus to deliver Auger emitters directly to the DNA of the target cells. The last-mentioned property is essential for the manifestation of cytotoxicity just by Auger electrons. No enhancement of anti-tumour activity was found for ^{125}I when it was delivered by internalizable antibodies into induced colorectal adenocarcinoma cells in athymic mice against the delivery of the same radionuclide by non-internalizable antibodies.[157] Therefore, the efforts of many laboratories are now concentrated on the development of internalizable vehicles that would be capable of delivering Auger emitters to the immediate vicinity of nuclear DNA.[158] Here, we will not consider vehicles that are efficient in cell culture experiments but cannot be applied at the body level.

Auger emitter vehicles can be divided into the following categories: (1) low-molecular-mass compounds; (2) natural oligopeptides and proteins, either unoptimized (unmodified) or optimized; and (3) artificial polypeptide and other macromolecular constructs. The last category includes modular nanotransporters, which will be considered in a special section below.

The low-molecular-mass compounds that constitute the first category include Auger-emitter-labelled oligonucleotides, steroids and some chemotherapeutic agents (for example, cisplatin and bleomycin). Comprehensive surveys [7, 158] over these compounds have recently been published, and the reader is referred to them.

Of the second-category vehicles, we should mention the extensive use of diverse peptide (polypeptide) ligands to an epidermal growth factor (EGF) receptor overexpressed on many types of cancer cells (glioblastoma, head and neck cancer, bladder cancer, esophageal cancer, *etc.*).[159, 160] There were attempts to use an EGF molecule itself as an

Auger emitter vehicle,[161, 162] although recent phase 1 clinical trials have not shown any anti-tumour effect of ^{111}In-DTPA-EGF.[163] This approach is based on the ability of an EGF receptor to translocate into the nuclei of normal and cancer cells (see, for example, surveys [164, 165]). However, the entire pool of internalizable EGF receptors (which is usually 10% – 30%) is far from appearing in the nuclei of all cells studied hitherto;[166, 167] in addition, the translocation of an EGF receptor into nucleus is affected by a set of diverse factors (see the survey [168]).‡ Nonetheless, attempts to modify various ligands to this receptor in order to optimize the intranuclear delivery of Auger emitters are continuing.[167, 169, 170]

The third category of vehicles comprises nuclisomes, that is, liposomes loaded with DNA intercalators, for example, daunorubicin derivatives labelled with Auger emitters.[171, 172] Specifically, nuclisomes where the constituent liposomes are modified by F5, a single-strand fragment of the variable region of anti-HER2 antibodies, and carry a ^{125}I-iodinated daunorubicin derivative, provided up to 70% survival rates in athymic mice with SKOV-3 human ovarian tumours.[172]

One more approach of this category employs polymeric vehicles [173, 174] that are sensitive to pH in the tumour. Vehicles were proposed that consisted of *N*-(2-hydroxypropyl)methacrylamide and *N*-(6-hydrazino-6-oxohexyl)-2-methylacrylamide methacrylamide copolymer and a 9-[^{125}I]iodoellipticine, a DNA intercalator attached thereto through an acid-sensitive linker. This construct was stable at pH 7.4; at pH 5.0, however, the iodinated intercalator separated out (in 44% yield in 24 h) [174] and acquired the opportunity to interact with the DNA. The underlying idea of the construct was the sensitivity of the linker to a reduction in pH; the authors proceeded from the documented observations of increased acidity in solid tumours. This construct increased the average lifespan of mice with transplanted mammary carcinoma 4T1 by 26.4% compared to the effect of free 9-[^{125}I]iodoellipticine and by 67.8% compared to the untreated control. Certainly, this approach suggests no cellular specificity of delivery.

We hold an opinion, as other researchers, too,[175 – 179] that modular nanotransporters are of considerable interest and have a good potential for use as delivery vehicles for both α-emitters and Auger emitters.

VIII. Modular nanotransporters: design and properties

A drug can be delivered to the nucleus if special transporters having tailored properties are designed to provide for the recognition of a target cell, the internalization of transporters loaded with the transported agent by the cell and their subsequent penetration into the nucleus. Modular transporters designed for this purpose [159, 180 – 184] comprised: (1) an internalizable ligand module to provide the recognition of the target cell and the subsequent receptor-mediated endocytosis of the transporter inward the cell; (2) an endosomolytic module to enable the transporter to leave endosomes; (3) a module having the nuclear localization sequence (NLS) to interact with importins, cytosolic proteins that ensure an active transfer into the nucleus; and (4) a carrier module to attach the delivered drug. The terms 'module' and 'modular' are here used in their direct meanings, as the transporter design took into account the possibility for the transporter to switch to various types of target cells and even different subcellular compartments, which can be attained more rapidly and smarter if transporter components are easily exchangeable (permutable). The need for several (at least four) components was dictated by the following reasoning. Firstly, a transporter can be endowed with cellular specificity simultaneously with the ability to penetrate inside the target cell if it comprises a component that has a high binding specificity to internalizable, endocytizable receptors. It is important that the receptors used be overexpessed on target cells and be weakly presented (in the ideal case, be absent) on normal cells nearby. Secondly, specific nuclear delivery is achievable when the transporter has an NLS. Thirdly, importins are cytosolic proteins, whereas the transporter, which entered the cell *via* receptor-mediated endocytosis, is enclosed in endocytic vesicles (endosomes and other) and is thereby separated from importins. This means that the transporter cannot interact with importins and it needs one more component to provide its escape from endocytic vesicles. Fourthly, all components, or modules, should be integrated into a single transporter and should have an opportunity to attach the transported drugs to the transporter; the carrier module serves for this purpose.

For the purposes of potential application, recombinant modular nanotransporters (MNTs) were bioengineered (their structures and stepped penetration into a cell are schematized in Fig. 3). They comprised (1) the α-melanocyte stimulating hormone (MSH) or EGF as internalizable ligand modules that are bound to type 1 melanocortin receptors overexpressed on human and murine melanoma cells, or EGF receptors overexpressed on head and neck, oesophageal cancer, bladder and other cancer cells; (2) an optimized NLS of the SV40 large T-antigen; (3) an *Escherichia coli* haemoglobin-like protein (HMP) as a carrier; and (4) the translocation domain of diphtheria toxin (DTox) as the endosomolytic module.[185 – 187] These MNTs were produced 95% – 98% pure. Modular nanotransporters having other ligand modules were designed later: with interleukin-3 (this MNT is targeted at acute myeloid leukaemia cells with the overexpression of interleukin-3 receptors) and with somatostatin (for neuroblastoma cells with somatostatin receptor overexpression).[188 – 190] Modular nanotransporters are denoted according to the sequence of their constituent modules from the N- to C-terminus, for example, as: DTox-HMP-NLS-MSH or DTox-HMP-NLS-EGF. The thus-prepared purified MNTs had molecular masses of ~70 kDa (varying depending on the MNT composition, specifically on the ligand module) and hydrodynamic diameters of 10.6 ± 0.5 nm.[191]

The modules in the MNT retained their functions necessary for fulfilling the major purpose, namely for providing specific intracellular drug delivery into target cells. Equilibrium dissociation constants (K_d) for complexes of MNTs with EGF receptors, such as HMP-NLS-DTox-EGF and DTox-HMP-NLS-EGF, were 40 and 29 nmol litre^{-1} respectively,[187] the values close to K_d for ^{125}I-EGF. The MSH, a 13-membered oligopeptide, had its affinity to melanocortin receptors slightly

‡ As to an insufficient efficacy of the nuclear delivery of Auger emitters into cells due to normal internalization of EGF receptor, also see Section IX.

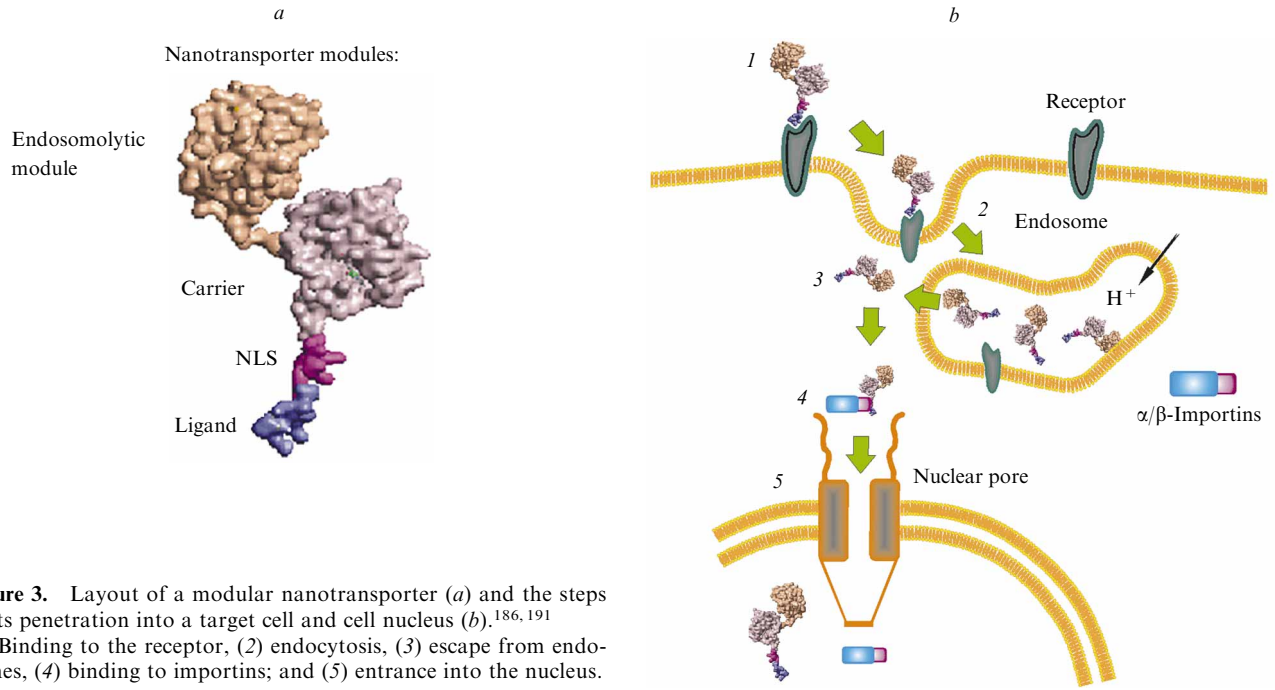


Figure 3. Layout of a modular nanotransporter (*a*) and the steps of its penetration into a target cell and cell nucleus (*b*).[186, 191] (*1*) Binding to the receptor, (*2*) endocytosis, (*3*) escape from endosomes, (*4*) binding to importins; and (*5*) entrance into the nucleus.

reduced when it entered MSH-comprising MNTs (to ~20 nmol litre^{-1}).[186]

The further fate of MNTs bound to internalizable receptors is determined by receptor-mediated endocytosis, the natural process of internalization, by the cell, of molecules (particles) specifically bound to receptors. Specifically, the MNT should appear in endosomes (closed-membrane vesicles with gradually acidified contents), which it should then actively leave to migrate to the cytosol, where importins, which can bind to the NLS to provide MNT delivery to the nucleus, are located. The escape from endosomes should be performed by the DTox endosomolytic module, whose purpose consists of generating defects in membranes on the side where the pH is weakly acidic (as inside the endosomes).

One method to evaluate the ability of a polypeptide to generate pores in membranes is to measure the dye leakage from dye-loaded liposomes. The tested MNTs caused dye leakage in two pH ranges. One range was 5.5 – 6.5, which is close to pH in endosomes and is due to the DTox module,[186, 187, 192] as it can itself generate pores in this range.[186] The other range was found at higher acidities, at pH ranging from 3 to 4, and was assigned to the effect of HMP.

MNT-generated membrane defects found in experiments on liposomes were characterized electrochemically and by atomic force microscopy.[187, 192, 193] The conductivity study of the planar lipid bilayer after MNT was added at pH 5.5 showed the emergence of ionic channels with conductivities of ~2 – 5 nS, whereas the MNT lacking an endosomolytic module had no this effect. Channels did not appear when the full-sized MNT performed in a neutral medium (pH 7.0). In 5 – 15 min after the medium was acidified to pH of 5.5, atomic force microscopy[187] detected ring structures 30 – 50 nm in diameter in the lipid bilayer (egg lecithin) in the presence of the MNT (Fig. 4). In 40 – 60 min, fluctuating holes having diameters of 50 – 200 nm and depths equal to the bilayer thickness were detected. At pH 7.0, no such modifications were detected. The fluctuating pores were shown to arise from two membrane-active domains (DTox and HMP). The diameters of these pores (50 – 200 nm) considerably exceeded the MNT sizes, so the MNT molecules unbound to the bilayer were likely to be capable of leaving endosomes and reaching their destination. Intriguingly, the DTox endosomolytic module when included into different MNT regions, yet caused the generation of identical defects in lipid membranes,[192] which implies its ability to function in various polypeptide contexts.

Atomic force microscopy with a modified probe showed that the elevations observed on the bilayer, which formed ring structures and were frequently seen near fluctuating pores, were built of MNT molecules. The MNT biospecificity of the cantilever tip of the atomic force microscope was achieved by modifying the tip with affinity-purified rabbit anti-MNT antibodies. This probe served to obtain curves where the interaction strength of the tip with the lipid bilayer and with the MNT on the lipid bilayer was plotted against the tip – object distance. The MNT – antibody specific interaction strength averaged 192 ± 23 pN, which is typical of antigen – antibody specific interactions.

When an antibody- or antigen-modified cantilever tip is used in tapping mode, a 1 – 2 nm increase is observed in the apparent height of scanned objects due to antigen – antibody interactions. When MNT-containing lecithin bilayers were scanned by an unmodified cantilever tip at pH 5.5, three types of species were detected with average heights of 1.1, 2.2 and 4.4 nm. Three types of species were also observed in scans when the cantilever tip was modified with anti-MNT antibodies. Their apparent heights were, however, reliably 1 – 2 nm higher: 2.0 [($p < 0.001$), 4.3 ($p < 0.05$) and 7 nm (p is the significance level of the statistic test). Therefore, all those species were formed by MNT molecules, and judging from their average heights, they were MNT molecules embedded into the bilayer, adsorbed on the bilayer surface and forming aggregates on the bilayer surface. These data provided an additional

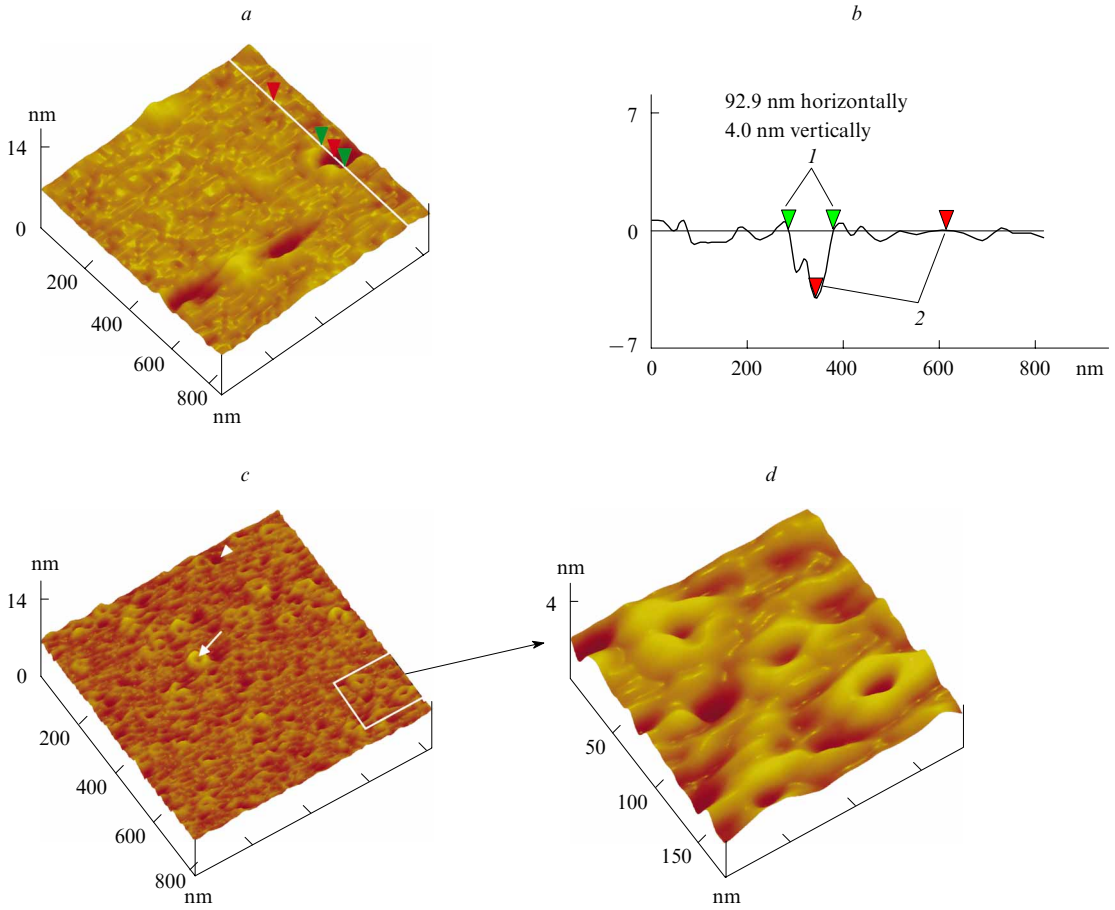


Figure 4. Defects in lipid bilayers caused by the DTox-HMP-NLS-EGF MNT at pH 5.5 as probed by atomic force microscopy.[187, 192] Images of large holes (*a*) and their section (*b*) by a normal plane along the white line with length (*1*) and width (*2*) characteristics; small defects (*c*) and their magnified image (*d*). One small defect surrounded by a torus is indicated by a white arrow; one large fluctuating hole is denoted by a white triangle.

characterization of MNTs. For example, analyzing ring structures, one could determine the average heights, widths and lengths of the MNT molecules embedded into the bilayer: 5.3 ± 0.4. 9.0 ± 0.9 and 12.5 ± 1.9 nm, respectively. These values and the average diameter of ring structures (43.1 ± 1.2 nm) made it possible to estimate the average number of MNT molecules in those structures at 11 ± 2.[191] It was inferred that, when the pH is acidified to 5.5, an MNT containing all the four modules, including the DTox endosomolytic module, can generate MNT-bordered pores in bilayers whose sizes will be sufficient for the MNTs to escape through them.

Finally, the functionality of the endosomolytic module was confirmed at the cellular level. Measurements of intracellular pH in the MNT microenvironment by image-ratio video microscopy [186] were used to elucidate the ability of an MNT comprising a DTox module to escape from acidified endocytosic compartments. In experiments on living murine Claudman S91 melanoma cells (clone M3), a truncated MNT version without endosomolytic module was detected in vesicles that had low-acidic or acidic contents, whereas the full-sized MNT (with the DTox module) was in neutral-pH microenvironment.

Surface plasmon resonance was used to characterize the interaction of the NLS in the MNT with an α/β-importin dimer:[187] the affinity constants of the studied MNTs to the importin dimer were very close to the constant of the natural polypeptide with the same NLS, which implied that this module was fully functional.

The location of full-sized MNTs inside the cell was almost exclusively intranuclear.[186, 187] Thus, all modules in the MNT retained their intrinsic functions to make it possible to fulfil the major purpose, *i.e.*, to deliver the MNT into the nucleus of the target cell.

IX. Modular nanotransporters as vehicles for the targeted nuclear delivery of α-particles and Auger electron emitters into target cells

As mentioned above, α-emitters and Auger electron emitters are most efficient in the cellular nucleus, so the dynamics of the nuclear content of the MNTs carrying these emitters is of special importance. The accumulation of an MNT that contains EGF as the ligand module (an MNT labelled by *N*-succinimidyl 3-[^{125}I]iodo-4-guanidinemethylbenzoate, [^{125}I]SGMIB-MNT), in the nuclei of human epidermoid carcinoma A431 cells reaches a maximum in 1 h after the cells were loaded with this MNT. Up to 60% of the radioactivity entering the cells appears in the nuclei.[194]

Astatine-211, which has a half-life of 7.2 h, was used as an MNT-delivered α-emitter. The first experiments [195] with ^{211}At used the modular polypeptide conjugates produced by joining the modules by bifunctional cross-linking agents. They showed the expected efficiency: a one-order-of-magnitude reduction in A_{37} (the radioactivity dose required to destroy 63% of the cells and thus leaving 37% of the cells alive) due to the nuclear delivery of ^{211}At to PLC/PRF/5 human hepatoma cells. Later [156] a recombinant MNT (DTox-HMP-NLS-EGF), labelled with ^{211}At with the use of *N*-succinimidyl 3-[^{211}At]astate-4-guanidino-4-methylbenzoate ([^{211}At]SAGMB), was used for the targeted damage of cancer cells with the EGF receptor overexpression, in human epidermoid carcinoma A431 and two human glioblastoma lines (D247 MG and U87MG.wtEGFR). Preliminary experiments showed that labelling did not modify the properties of the MNT. Cell survival tests clearly showed a more pronounced cytotoxicity of [^{211}At]SAGMB-MNT compared to free ^{211}At in all three cancer cell lines. For glioblastoma D247 MG cells (Fig. 5), A_{37} values for [^{211}At]SAGMB-MNT and unbound ^{211}At were 3.8 and 69 kBq ml^{-1}, respectively. In other words, the nuclear delivery of ^{211}At to the target cells increased its cytotoxicity by a factor of 18.2. For the other two lines, A431 and U87MG.wtEGFR, the gain in cytotoxicity was 14.5 and 8.3 times, respectively. Later quantitative calculations implied that the recoil nuclei generated by α-decay of ^{211}At contributed to the [^{211}At]SGMAB-MNT overall effect.[156]

Iodine-125 and gallium-67, the isotopes emitting on the average 20 and 5 Auger electrons, respectively, per decay, were used as MNT-delivered Auger emitters. The MNT-transported iodine-125 ([^{125}I]SGMIB-MNT) was 3500 times more potent in damaging human epidermoid carcinoma cells A431 (Fig. 6) than iodine-125 was in the control polypeptide, which was incapable of penetrating cell nuclei.[194] Koumarianou *et al.*[196] obtained qualitatively similar results for gallium-67 (Table 9).

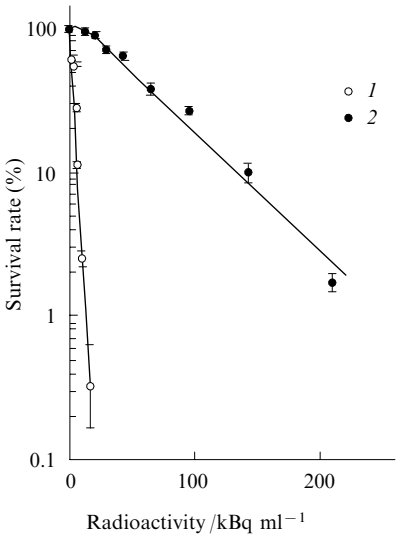


Figure 5. Survival rate (scored as the colony-forming ability) of glioblastoma D247 MG cells with various radioactivities of astatine-211 added as [^{211}At]SAGMB-MNT (*1*) or free 211-astatine (*2*).[156]

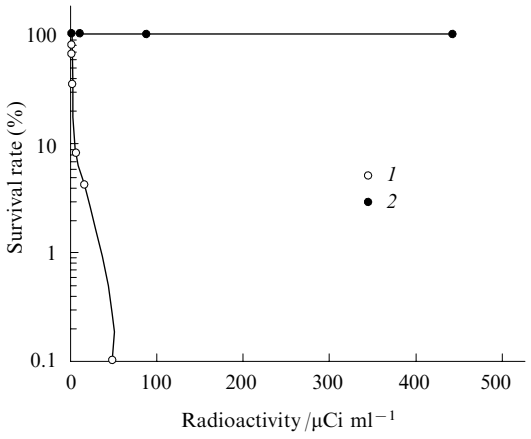


Figure 6. Enhancement of cell death rate (scored as the colony-forming ability) of human adenocarcinoma A431 cells induced by the ^{125}I Auger electron emitter delivered by DTox-HMP-NLS-EGF-[^{125}I]SGMIB MNT (*1*).[192]
The control is ^{125}I loaded to bovine serum albumin (BSA), which cannot penetrate cells and their nuclei (*2*).

In both studies,[194, 196] the efficacy of MNT-delivered Auger emitters targeted at cancer cells with EGF receptor overexpression, was compared against the efficacy of the same Auger emitters (^{125}I and ^{67}Ga) attached to EGF. The MNT-delivered ^{125}I and ^{67}Ga had cytotoxicities about one order of magnitude higher than the EGF-delivered species had: in terms of A_{37}, cytotoxicity increased by a factor of 5 and 13 for ^{125}I and ^{67}Ga, respectively; in terms of A_{10} (the dose that left alive 10% cells), the gain in cytotoxicity was 18 times for both Auger emitters.[194, 196] We may infer that the mere binding to an EGF receptor is insufficient for providing a high cytotoxicity of Auger emitters. Likely, it is necessary to endow the Auger emitter delivery vehicle both with the possibility to escape from endocytosic compartments and with NLS, *i.e.*, with the modules that are present in the MNT.

Modular nanotransporters appeared to be of low toxicity to mice. C57 black/6J mice tolerated the maximal achievable dose of intravenous DTox-HMP-NLS-MSH (7.5 mg); higher doses were unachievable because of intravenously administered volume limitations and MNT solubility. C57 black/6J mice and Balb/c ByJIco-*nu*/*nu* immunodeficient mice were able to tolerate multiple intravenous administrations of four times of 2 mg DTox-HMP-NLS-MSH and six times of 3 mg DTox-HMP-NLS-EGF, respectively, with 2 – 3 day intervals between injections. The

Table 9. Comparative cytotoxicity (in terms of A_{37} and A_{10}) of ^{67}Ga delivered with an MNT into cancer cell nuclei against other vehicles.[196]

Cell line	^{67}Ga vehicle (other than MNT)	A_{37} (MNT) : A_{37} (vehicle)	A_{10} (MNT) : A_{10} (vehicle)
Human epidermoid carcinoma A431	EGF	13	18
	BSA	17	17
	EDTA	385	388
Human glioblastoma WTT	EGF	72	18

intravenous administration of DTox-HMP-NLS-EGF to C57 black/6J mice in a dose of 4 mg did not cause any significant behavioural modification or macroscopic alterations of organs in these mice compared to the control animals, which received physiological saline.[191]

The selectivity of accumulation of labelled MNTs in B16-F1 tumour transferred to mice C57Black/6J increased considerably as the MNT dose reached the ratios 13.4 ± 1.7 (tumour : muscle) and 9.8 ± 1.8 (tumour : skin) as soon as in 3 h post intravenous administration.[191, 197]

The distribution (target cells: melanoma) of the DTox-HMP-NLS-MSH MNT upon intravenous administration to mice bearing Claudman melanoma S91 (clone M3) elucidated the preferred accumulation of the MNT in cancer cells, and in nuclei inside the cells. A similar result was obtained after immunodeficient mice having epidermoid carcinoma were administered with another MNT, namely DTox-HMP-NLS-EGF, which is targeted at epidermoid carcinoma cells and some other cancer cells (see above) (Fig. 7).[191]

In vivo experiments with the delivery of Auger emitters have not yet been published, so we will briefly review the information published on the enhancement of the antitumour effect of photosensitizers (PSs) delivered to cancer cell nuclei of experimental tumours. Photosensitizer-generated reactive oxygen species (which are real active cytotoxic agents) are known to have very short ranges, which is a common feature of the action of photosensitizers and the effects caused by α-emitters and Auger emitters. Unlike the latter, the production of reactive oxygen species by photosensitizers can be switched on or off almost instantaneously by manipulating the light absorbed by the photosensitizer.

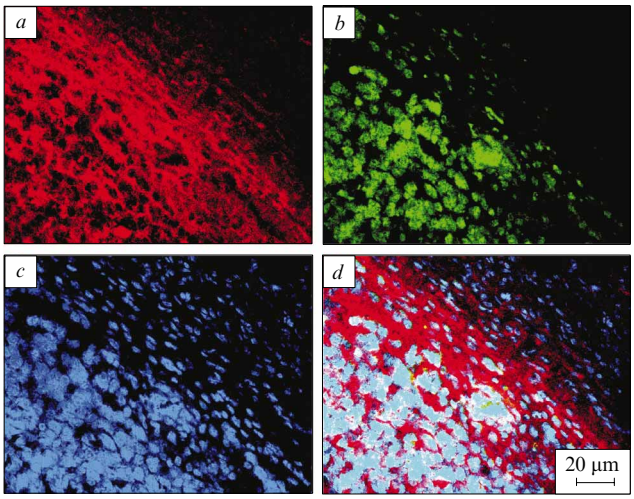


Figure 7. Immunofluorescent detection of the DTox-HMP-NLS-MSH MNT in the tumour and surrounding tissue 3 h post intravenous administration to DBA line mice with Claudman S91 (clone M3) melanoma constantly transformed by the green fluorescent protein gene.[191]
(*a*–*d*) Tumour surrounding tissue: (*a*) the MNT detected by AlexaFluor 555 staining (red fluorescence); (*b*) Claudman S91 (clone M3) melanoma cancer cells with green fluorescent protein (green fluorescence); (*c*) all cellular nuclei stained with 4′,6-diamidino-2-phenylindole; and (*d*) superposition of figures (*a*), (*b*) and (*c*).

Experiments were performed on immunodeficient mice with transplanted human epidermoid carcinoma. The 98% tumour growth inhibition was found when the chlorin e_6 photosensitizer was delivered by the DTox-HMP-NLS-EGF MNT. All untreated animals died by day 24 post tumour transplantation, against the 75% survival observed in the tumour-carrying mice treated with the MNT-delivered photosensitizer (Fig. 8). For comparison: in the control that was treated with the photosensitizer alone (without MNT-assisted delivery), the animal survival rate was as low as 20% (in the experiment and control on observation day 92).[191]

A significant increase in the cytotoxicity of the bacteriochlorin *p* photosensitizer was found in Claudman S91 (clone M3) and B16-F1 melanoma models. A reliable increase in tumour growth inhibition and in the average survival time of tumour-carrying animals was found upon treatment with the MNT-delivered photosensitizer against the effect caused by the photosensitizer alone. The effect was more pronounced in model less pigmented melanoma Claudman S91 (clone M3).[197]

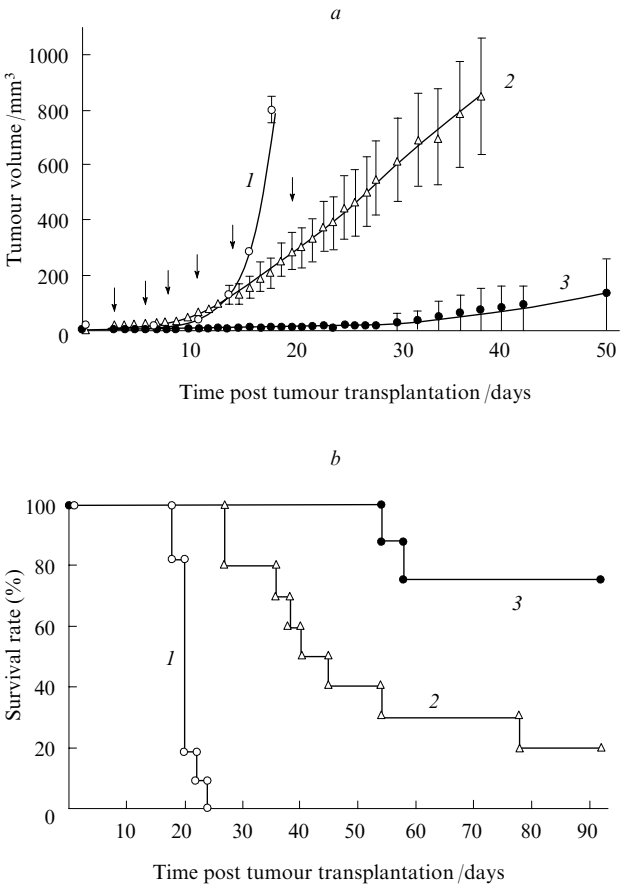


Figure 8. Tumour growth inhibition (*a*) and a noticeable gain in survival rate (*b*) in immunodeficient mice with transplanted human epidermoid carcinoma upon photodynamic therapy.[191]
(*1*) Control, (*2*) free PS, and (*3*) MNT-transported PS. Arrows indicate the PS and PS-MNT administration times and subsequent irradiation time (PS is chlorin e_6).

X. Conclusion

The efficacy of a radiopharmaceutical agent is determined by the combination of nuclear-physical properties of the radionuclide and the biochemical behaviour of its delivery vehicles. The use of MNTs, which deliver the radionuclide into the cancer cell nucleus, makes it possible to enhance the cytotoxic effect of α-emitters and especially of Auger electron emitters. The delivery of ^{211}At to the nuclei of target cells increased its cytotoxicity by a factor ranging from 8.3 to 18.2. For ^{67}Ga, the use of MNTs increased cytotoxicity by one to two orders of magnitude, and for ^{125}I, by three orders of magnitude.

We may expect that the application of MNTs as delivery vehicles will greatly expand the range of therapeutic radionuclides to include emitters of low-energy (Auger and conversion) electrons. Well-known diagnostic radionuclides (^{111}In and ^{67}Ga), for which methods for production, separation, and incorporation into biomolecules have been developed, can be used in this new quality. Importantly, their use will not require an appreciable expansion of the existing park of accelerators.

Apart from the above-listed radionuclides, some lanthanide radionuclides (^{165}Er, ^{167}Tm, *etc.*) and platinum-metal radionuclides (^{191}Pt, ^{193m}Pt, ^{195m}Pt), which have attractive nuclear-physical and chemical properties, are expected to enter practice in the more distant future. However, for them to be applied widely, more research into their nuclear properties and into the coordination chemistry and radiochemistry of those elements is necessary.

Phase 2 clinical trials of several agents comprising α-emitters, such as ^{211}At, ^{212}Pb/^{212}Bi, ^{213}Bi and ^{225}Ac, for use in cancer radioimmunotherapy are now underway; therefore, drugs of this group can enter the market in the near future.

Unfortunately, the applications of α-emitters are hindered by serious production challenges (for ^{211}At and ^{225}Ac), short half-lives (for ^{212}Bi and ^{213}Bi), daughter emitters in the chain (for ^{212}Pb and ^{225}Ac), or an insufficient stability of bioconjugates in the body (for ^{211}At). Modular nanotransporters help to partially solve the problem of daughter radionuclides due to the delivery of the parent nucleus inside cancer cells to hinder subsequent proliferation of daughter nuclei.

Despite the active search for alternatives, today the main way of getting ^{225}Ac is still release from old ^{233}U. The latest studies showed the feasibility of large-scale ^{225}Ac production on accelerators of moderate-energy electrons, but there are few such accelerators in the world. The thus-prepared product contains a ^{227}Ac impurity, so it can be used only in the manufacture of ^{213}Bi generators. Thus, technical difficulties associated with the production of ^{213}Bi can generally be considered as resolved.

It seems likely that nuclear therapy will gradually turn from reactor-produced radionuclides to accelerator-produced radionuclides to solve the problem of low specific activities typical of many reactor-produced nuclides. In addition, production on accelerator facilities satisfies nuclear safety requirements to a greater extent.

This survey was prepared with financial support by the Russian Science Foundation (Project No. 14-14-00874) and the Russian Foundation for Basic Research (Project No. 13-03-01304).

References

1. C Regaud, A Lacassagne, in *Archives de l'Institut du Radium de l'Universitg de Paris et La Fondation Curie. Radiophysiologie et Radiotherapie, Paris, 1927* p. 95
2. S H Britz-Cunningham, S J Adelstein *J. Nucl. Med.* **44** 1945 (2003)
3. S Huclier-Markai, C Alliot, N Varmenot, C S Cutler, J Barbet *Curr. Top. Med. Chem.* **12** 2642 (2012)
4. A A S Tavares, J M R S Tavares *Int. J. Radiat. Biol.* **86** 261 (2010)
5. S L Kitson *Cancer Stud. Mol. Med. Open J.* **1** 8 (2014)
6. A I Kassis *J. Nucl. Med.* **44** 1479 (2003)
7. C R T Hillyar, B Cornelissen, K A Vallis *Ther. Deliv.* **5** 319 (2014)
8. S DeNardo, J A Jungerman, G L DeNardo, M C Lagunas-Solar, W C Cole, C F Meares, in *The Developing Role of Short-Lived Radionuclides in Nuclear Medical Practice (Proceedings of the Inernationsl Symposium, Washington, May 3 – 5, 1982)* (Eds P Paras, J W Thiessen) (Washington, DC, 1985) p. 401
9. S C Srivastava *Cancer Biother. Radiopharm.* **11** 43 (1996)
10. L F Mausner, S C Srivastava *Med. Phys.* **20** 503 (1993)
11. P Hoskin, O Sartor, J M O'Sullivan, D C Johannessen, S I Helle, J Logue, D Bottomley, S Nilsson, N J Vogelzang, F Fang, M Wahba, A-K Aksnes, C Parker *Lancet Oncol.* **15** 1397 (2014)
12. S Nilsson, in *American Society of Clinical Oncology Educational Book* (Alexandria, VA: ASCO, 2014) p. e132
13. C J Ryan, P J Saylor, J J Everly, O Sartor *Oncologist* **19** 1012 (2014)
14. P G Turner, J O'Sullivan *Expert Opin. Pharmacother.* **15** 2105 (2014)
15. H A Wieder, M Lassmann, M S Allen-Auerbach, J Czernin, K Herrmann *World J. Radiol.* **6** 480 (2014)
16. A Morgenstern, L Krolícki, J Kunikowska, H Koziara, B Królicki, M Jakuciński, C Apostolidis, F Bruchertseifer *J. Nucl. Med.* **55** (Suppl. 1) Paper No. 390 (2014)
17. L Królicki, A Morgenstern, J Kunikowska, H Koziara, B Królicki, M Jakuciński, C Apostolidis, F Bruchertseifer *Eur. J. Nucl. Med. Mol. Imag.* **41** (Suppl. 2) S291 (Abstract OP603) (2014)
18. C Kratochwil, F L Giesel, F Bruchertseifer, W Mier, C Apostolidis, R Boll, K Murphy, U Haberkorn, A Morgenstern *Eur. J. Nucl. Med. Mol. Imag.* **41** 2106 (2014)
19. L S Yasui *Int. J. Radiat. Biol.* **88** 864 (2012)
20. Y-S Kim, M W Brechbiel *Tumour Biol.* **33** 573 (2012)
21. N Falzone, B Cornelissen, K A Vallis, in *Radiation Damage in Biomolecular Systems* (Eds G García Gómez-Tejedor, M C Fuss) (Springer, 2012) p. 461
22. C Seidl *Immunotherapy* **6** 431 (2014)
23. B J Allen, C Y Huang, R A Clarke *Biologics: Targets, Ther.* **8** 255 (2014)
24. O Sartor, B N Maalouf, C R Hauck, R M Macklis *J. Nucl. Med. Radiat. Ther.* **3** Art. No. 136 (2012)
25. W D Bloomer, S J Adelstein *Pathobiol. Annu.* **8** 407 (1978)
26. W D Bloomer, S J Adelstein *Curr. Top. Radiat. Res. Quart.* **12** 513 (1978)
27. P C Chan, E Lisco, H Lisco, S J Adelstein *Radiat. Res.* **67** 332 (1976)
28. S L Commerford, V P Bond, E P Cronkite, U Reincke *Int. J. Radiat. Biol. Relat. Stud. Phys. Chem. Med.* **37** 547 (1980)

29. R Alberto, in *Topics in Organometallic Chemistry* Vol. 32 (Eds G Jaouen, N Metzler-Nolte) (Springer, 2010) p. 219
30. Y-Y Hsiao, T-H Hung, S-J Tu, C-J Tung *Int. J. Radiat. Biol.* **90** 392 (2014)
31. A I Kassis, S J Adelstein *J. Nucl. Med.* **46** (Suppl. 1) 4S (2005)
32. A I Kassis *Int. J. Radiat. Biol.* **80** 789 (2004)
33. P Balagurumoorthy, X Xu, K Wang, S J Adelstein, A I Kassis *Int. J. Radiat. Biol.* **88** 998 (2012)
34. S M Goddu, R W Howell, D V Rao *J. Nucl. Med.* **35** 303 (1994)
35. J L Humm, R W Howell, D V Rao *Med. Phys.* **21** 1901 (1994)
36. S Y F Chu, L P Ekström, R B Firestone *The Lund/LBNL Nuclear Data Search Database* (1999); http://nucleardata.nuclear.lu.se/toi/index.asp
37. S M Qaim, F T Tarkanyi, P Oblozinsky, K Gul, A Hermanne, M G Mustafa, F M Nortier, B Scholten, Yu Shubin, S Takacs, Y Zhuang *Charged Particle Cross-Section Database for Medical Radioisotope Production: Diagnostic Radioisotopes and Monitor Reactions* IAEA-TECDOC-1211, Vienna, 2001; http://www-nds.iaea.org/medical/index.html
38. F Szelecsényi, T E Boothe, E Tavano, M E Plitnikas, F Tárkányi *Appl. Radiat. Isot.* **45** 473 (1994)
39. M U Khandaker, H Haba, M Murakami, N Otuka *Nucl. Instrum. Methods Phys. Res., Sect. B* **346** 8 (2015)
40. M N Aslam, S Sudár, M Hussain, A A Malik, S M Qaim *Appl. Radiat. Isot.* **69** 1490 (2011)
41. H E Hassan, S M Qaim, Yu Shubin, A Azzam, M Morsy, H H Coenen *Appl. Radiat. Isot.* **60** 899 (2004)
42. G Blessing, R Weinreich, S M Qaim, G Stöcklin *Int. J. Appl. Radiat. Isot.* **33** 333 (1982)
43. K Gagnon, F Bénard, M Kovacs, T J Ruth, P Schaffer, J S Wilson, S A McQuarrie *Nucl. Med. Biol.* **38** 907 (2011)
44. G Pupillo, J Esposito, M Gambaccini, F Haddad, N Michel *J. Radioanal. Nucl. Chem.* **302** 911 (2014)
45. S Takács, A Hermanne, F Tárkányi, A Ignatyuk *Nucl. Instrum. Methods Phys. Res., Sect. B* **268** 2 (2010)
46. H Thisgaard, PhD Thesis, Technical University of Denmark, Roskilde, Denmark, 2008 (Risu-PhD-42)
47. H Thisgaard, M Jensen *Appl. Radiat. Isot.* **67** 34 (2009)
48. F Tárkányi, S M Qaim, G Stöcklin, M Sajjad, R M Lambrecht, H Schweickert *Int. J. Radiat. Appl. Instrum., Part A: Appl. Radiat. Isot.* **42** 221 (1991)
49. B Scholten, Z Kovács, F Tárkányi, S M Qaim *Appl. Radiat. Isot.* **46** 255 (1995)
50. J A Nye, M A Avila-Rodriguez, R J Nickles *Appl. Radiat. Isot.* **65** 407 (2007)
51. A Hohn, F M Nortier, B Scholten, T N van der Walt, H H Coenen, S M Qaim *Appl. Radiat. Isot.* **55** 149 (2001)
52. M N Aslam, S Sudár, M Hussain, A A Malik, H A Shah, S M Qaim *Appl. Radiat. Isot.* **68** 1760 (2010)
53. K Hilgers, Yu N Shubin, H H Coenen, S M Qaim *Radiochim. Acta* **93** 553 (2005)
54. F Rösch, J Brockmann, N A Lebedev, S M Qaim *Acta Oncol.* **39** 727 (2000)
55. F Tárkányi, A Hermanne, S Takács, F Ditrói, B Király, S F Kovalev, A V Ignatyuk *Nucl. Instrum. Methods Phys. Res., Sect. B* **266** 3346 (2008)
56. F Tárkányi, A Hermanne, S Takács, F Ditrói, B Király, S F Kovalev, A V Ignatyuk *Nucl. Instrum. Methods Phys. Res., Sect. B* **266** 3529 (2008)
57. F Tárkányi, A Hermanne, S Takács, B Király, I Spahn, A V Ignatyuk *Appl. Radiat. Isot.* **68** 250 (2010)
58. F Tárkányi, A Hermanne, B Király, S Takács, A V Ignatyuk *Appl. Radiat. Isot.* **68** 404 (2010)
59. F Tárkányi, B Király, F Ditrói, S Takács, J Csikai, A Hermanne, M S Uddin, M Hagiwara, M Baba, T Ido, Yu N Shubin, A I Dityuk *Nucl. Instrum. Methods Phys. Res., Sect. B* **239** 293 (2005)
60. F Tárkányi, B Király, F Ditrói, S Takács, J Csikai, A Hermanne, M S Uddin, M Hagiwara, M Baba, Yu N Shubin, S F Kovalev *Nucl. Instrum. Methods Phys. Res., Sect. B* **247** 210 (2006)
61. F Groppi, C Birattari, M Bonardi, M Gallorini, L Gini *J. Radioanal. Nucl. Chem.* **249** 289 (2001)
62. M Bonardi, C Birattari, M Gallorini, F Groppi, D Arginelli, L Gini *J. Radioanal. Nucl. Chem.* **236** 159 (1998)
63. S M Qaim, K Hilgers, S Sudár, H H Coenen *Appl. Radiat. Isot.* **67** 1074 (2009)
64. M S Uddin, B Scholten, A Hermanne, S Sudár, H H Coenen, S M Qaim *Appl. Radiat. Isot.* **68** 2001 (2010)
65. P P Dmitriev *Vykhod Radionuklidov v Reaktsiyakh s Protonami, Deitronami, Al'fa-chastitsami i Geliem-3* (Radionuclide Yield of Reactions with Protons, Deuterons, Alpha-Particles and Helium-3) (Moscow: Energoatomizdat, 1986)
66. R Adam Rebeles, A Hermanne, P Van den Winkel, F Tvrkvnyi, S Takvcs *J. Korean Phys. Soc.* **59** 1975 (2011)
67. M S Uddin, M U Khandaker, K S Kim, Y S Lee, G N Kim *Nucl. Instrum. Methods Phys. Res., Sect. B* **258** 313 (2007)
68. F Groppi, M L Bonardi, C Birattari, L Gini, C Mainardi, E Menapace, K Abbas, U Holzwarth, R M F Stroosnijder *Nucl. Instrum. Methods Phys. Res., Sect. B* **213** 373 (2004)
69. J H Kim, H Park, K S Chun *Appl. Radiat. Isot.* **68** 1623 (2010)
70. J W Engle, V Lopez-Rodriguez, R E Gaspar-Carcamo, H F Valdovinos, M Valle-Gonzalez, F Trejo-Ballado, G W Severin, T E Barnhart, R J Nickles, M A Avila-Rodriguez *Appl. Radiat. Isot.* **70** 1792 (2012)
71. G Blessing, S M Qaim *Int. J. Appl. Radiat. Isot.* **35** 927 (1984)
72. V Tolmachev, A Lövqvist, L Finarsson, J Schultz, H Lundqvist *Appl. Radiat. Isot.* **49** 1537 (1998)
73. T J Ruth *J. Nucl. Med. Technol.* **42** 245 (2014)
74. C S Cutler, S W Schwarz *J. Nucl. Med.* **55** 1208 (2014)
75. S C van der Marck, A J Koning, K E Charlton *Eur. J. Nucl. Med. Mol. Imag.* **37** 1817 (2010)
76. B Wolterbeek, J L Kloosterman, D Lathouwers, M Rohde, A Winkelman, L Frima, F Wols *J. Radioanal. Nucl. Chem.* **302** 773 (2014)
77. M U Khandaker, K Kim, M W Lee, K S Kim, G N Kim, Y S Cho, Y O Lee *Nucl. Instrum. Methods Phys. Res., Sect. B* **266** 4877 (2008)
78. A Hermanne, R Adam Rebeles, P Van den Winkel, F Tárkányi, S Takács *Nucl. Instrum. Methods Phys. Res., Sect. B* **339** 26 (2014)
79. F Tárkányi,, B Király, F Ditrói, S Takács, J Csikai, A Hermanne, M S Uddin, M Hagiwara, M Baba, T Ido, Yu N Shubin, S F Kovalev *Nucl. Instrum. Methods Phys. Res., Sect. B* **259** 817 (2007)
80. V I Levin *Poluchenie Radioaktivnykh Izotopov* (Production of Radioactive Isotopes) (Moscow: Atomizdat, 1972)
81. A Hermanne, R Adam-Rebeles, P Van den Winkel, F Tárkányi, S Takács *Radiochim. Acta* **102** 1111 (2014)
82. H Thisgaard, M Jensen *Med. Phys.* **35** 3839 (2008)
83. S M Qaim *Radiochim. Acta* **89** 189 (2001)

84. F Tárkányi, S Takács, B Király, F Szelecsényi, L Andó, J Bergman, S-J Heselius, O Solin, A Hermanne, Yu N Shubin, A V Ignatyuk *Appl. Radiat. Isot.* **67** 1001 (2009)
85. G J Beyer, S K Zeisler, D W Becker *Radiochim. Acta* **92** 219 (2004)
86. F Tárkányi, A Hermanne, S Takács, F Ditrói, B Király, H Yamazaki, M Baba, A Mohammadi, A V Ignatyuk *Nucl. Instrum. Methods Phys. Res., Sect. B* **267** 2789 (2009)
87. F Tárkányi, A Hermanne, B Király, S Takács, F Ditrói, M Baba, T Ohtsuki, S F Kovalev, A V Ignatyuk *Nucl. Instrum. Methods Phys. Res., Sect. B* **259** 829 (2007)
88. K Hilgers, H H Coenen, S M Qaim *Appl. Radiat. Isot.* **66** 545 (2008)
89. M P Dykiy, A N Dovbnya, Yu V Lyashko, E P Medvedeva, D V Medvedev, V L Uvarov *J. Label. Compd. Radiopharm.* **50** 480 (2007)
90. S Takács, F Tárkányi, A Hermanne *Nucl. Instrum. Methods Phys. Res., Sect. B* **240** 790 (2005)
91. F Tárkányi, F Ditrói, A Hermanne, S Takács, R Adam-Rebeles, N Walravens, O Cichelli, A V Ignatyuk *Appl. Radiat. Isot.* **74** 109 (2013)
92. E Lebowitz, M W Greene, R Fairchild, P R Bradley-Moore, H L Atkins, A N Ansari, P Richards, E Belgrave *J. Nucl. Med.* **16** 151 (1975)
93. S M Qaim, R Weinreich, H Ollig *Int. J. Appl. Radiat. Isot.* **30** 85 (1979)
94. A Hermanne, N Walravens, O Cicchelli, in *Nuclear Data for Science and Technology (Research Reports in Physics)* (Ed. S M Qaim) (Springer, 1992) p. 616
95. R Adam Rebeles, P Van den Winkel, A Hermanne, F Tárkányi, S Takács *Nucl. Instrum. Methods Phys. Res., Sect. B* **288** 94 (2012)
96. A Azzam, S A Said, M Al-abyad *Appl. Radiat. Isot.* **91** 109 (2014)
97. M W Brechbiel *Dalton Trans.* 4918 (2007)
98. O Couturier, S Supiot, M Degraef-Mougin, A Faivre-Chauvet, T Carlier, J-F Chatal, F Davodeau, M Cherel *Eur. J. Nucl. Med. Mol. Imag.* **32** 601 (2005)
99. N A P Franken, S Hovingh, R Ten Cate, P Krawczyk, J Stap, R Hoebe, J Aten, G W Barendsen *Oncol. Rep.* **27** 769 (2012)
100. A K Claesson, B Stenerlöw, L Jacobsson, K Elmroth *Radiat. Res.* **167** 312 (2007)
101. C Wulbrand, C Seidl, F C Gaertner, F Bruchertseifer, A Morgenstern, M Essler, R Senekowitsch-Schmidtke *PLoS One* **8** e64730 (2013)
102. M Essler, F C Gärtner, F Neff, B Blechert, R Senekowitsch-Schmidtke, F Bruchertseifer, A Morgenstern, C Seidl *Eur. J. Nucl. Med. Mol. Imag.* **39** 602 (2012)
103. C Müller, J Reber, S Haller, H Dorrer, U Köster, K Johnston, K Zhernosekov, A Türler, R Schibli *Pharmaceuticals* **7** 353 (2014)
104. G F Steyn, C Vermeulen, F Szelecsényi, Z Kovács, A Hohn, N P van der Meulen, R Schibli, T N van der Walt *Nucl. Instrum. Methods Phys. Res., Sect. B* **319** 128 (2014)
105. M R Zalutsky, M Pruszynski *Curr. Radiopharm.* **4** 177 (2011)
106. A Hermanne, F Tárkányi, S Takács, Z Szücs, Yu N Shubin, A I Dityuk *Appl. Radiat. Isot.* **63** 1 (2005)
107. O Lebeda, R Jiran, J Ráliš, J Štursa *Appl. Radiat. Isot.* **63** 49 (2005)
108. G Henriksen, S Messelt, E Olsen, R H Larsen *Appl. Radiat. Isot.* **54** 839 (2001)
109. A T Yordanov, O Pozzi, S Carlin, G Akabani, B Wieland, M R Zalutsky *J. Radioanal. Nucl. Chem.* **262** 593 (2004)
110. C Alliot, M Chérel, J Barbet, T Sauvage, G Montavon *Radiochim. Acta* **97** 161 (2009)
111. D Wild, M Frischknecht, H Zhang, A Morgenstern, F Bruchertseifer, J Boisclair, A Provencher-Bolliger, J-C Reubi, H R Maecke *Cancer Res.* **71** 1009 (2011)
112. C Apostolidis, R Molinet, G Rasmussen, A Morgenstern *Anal. Chem.* **77** 6288 (2005)
113. B Zielinska, C Apostolidis, F Bruchertseifer, A Morgenstern *Solv. Extract. Ion Exchange* **25** 339 (2007)
114. R A Boll, D Malkemus, S Mirzadeh *Appl. Radiat. Isot.* **62** 667 (2005)
115. A Morgenstern, F Bruchertseifer, C Apostolidis *Curr. Radiopharm.* **4** 295 (2011)
116. L I Guseva *Radiochemistry* **56** 451 (2014) [*Radiokhimiya* **56** 385 (2014)]
117. M W Geerlings, F M Kaspersen, C Apostolidis, R van der Hout *Nucl. Med. Commun.* **14** 121 (1993)
118. V A Khalkin, V V Tsupko-Sitnikov, N G Zaitseva *Radiokhimiya* **39** 481 (1997)
119. Patent RF 2199165 (2001)
120. C Apostolidis, R Molinet, J McGinley, K Abbas, J Möllenbeck, A Morgenstern *Appl. Radiat. Isot.* **62** 383 (2005)
121. G Melville, P Melville *Appl. Radiat. Isot.* **72** 152 (2013)
122. O D Maslov, A V Sabel'nikov, S N Dmitriev *Radiochemistry* **48** 195 (2006) [*Radiokhimiya* **48** 176 (2006)]
123. G Melville, B J Allen *Appl. Radiat. Isot.* **67** 549 (2009)
124. G Melville, H Meriarty, P Metcalfe, T Knittel, B J Allen *Appl. Radiat. Isot.* **65** 1014 (2007)
125. G Melville, S F Liu, B J Allen *Appl. Radiat. Isot.* **64** 979 (2006)
126. B L Zhuikov, S N Kalmykov, S V Ermolaev, R A Aliev, V M Kokhanyuk, V L Matushko, I G Tananaev, B F Myasoedov *Radiochemistry* **53** 73 (2011) [*Radiokhimiya* **53** 66 (2011)]
127. S V Ermolaev, B L Zhuikov, V M Kokhanyuk, V L Matushko, S N Kalmykov, R A Aliev, I G Tananaev, B F Myasoedov *Radiochim. Acta* **100** 223 (2012)
128. J W Weidner, S G Mashnik, K D John, F Hemez, B Ballard, H Bach, E R Birnbaum, L J Bitteker, A Couture, D Dry, M E Fassbender, M S Gulley, K R Jackman, J L Ullmann, L E Wolfsberg, F M Nortier *Appl. Radiat. Isot.* **70** 2602 (2012)
129. J W Weidner, S G Mashnik, K D John, B Ballard, E R Birnbaum, L J Bitteker, A Couture, M E Fassbender, G S Goff, R Gritzo, F M Hemez, W Runde, J L Ullmann, L E Wolfsberg, F M Nortier *Appl. Radiat. Isot.* **70** 2590 (2012)
130. J W Engle, J W Weidner, B D Ballard, M E Fassbender, L A Hudston, K R Jackman, D E Dry, L E Wolfsberg, L J Bitteker, J L Ullmann, M S Gulley, C Pillai, G Goff, E R Birnbaum, K D John, S G Mashnik, F M Nortier *Radiochim. Acta* **102** 569 (2014)
131. R A Aliev, S V Ermolaev, A N Vasiliev, V S Ostapenko, E V Lapshina, B L Zhuikov, N V Zakharov, V V Pozdeev, V M Kokhanyuk, B F Myasoedov, S N Kalmykov *Solv. Extract. Ion Exchange* **32** 468 (2014)
132. A Morgenstern, F Bruchertseifer, C Apostolidis *Curr. Radiopharm.* **5** 221 (2012)
133. L I Guseva, N N Dogadkin *J. Radioanal. Nucl. Chem.* **285** 667 (2010)

134. L I Guseva, N N Dogadkin *Radiochemistry* **51** 169 (2009) [*Radiokhimiya* **51** 148 (2009)]
135. M L Dietz, E F Horwitz *Ind. Eng. Chem. Res.* **39** 3181 (2000)
136. C Wu, M W Brechbiel, O A Gansov *Radiochim. Acta* **79** 141 (1997)
137. M R McDevitt, R D Finn, G Sgouros, D Ma, D A Scheinberg *Appl. Radiat. Isot.* **50** 895 (1999)
138. M R McDevitt, R D Finn, D Ma, S M Larson, D A Scheinberg *J. Nucl. Med.* **40** 1722 (1999)
139. D Ma, M R McDevitt, R D Finn, D Scheinberg *Appl. Radiat. Isot.* **55** 667 (2001)
140. W Wrasidlo, K J Mysels *Colloids Surf., A: Physicochem. Eng. Aspects* **186** 123 (2001)
141. A Le Du, M Mougin-Degraef, E Botosoa, A Rauscher, A Faivre Chauvet, J Barbet, G Montavon *Radiochim. Acta* **99** 743 (2011)
142. L I Guseva *Radiochemistry* **52** 270 (2010) [*Radiokhimiya* **52** 229 (2010)]
143. L I Guseva *J. Radioanal. Nucl. Chem.* **272** 153 (2007)
144. National Nuclear Data Center, Brookhaven National Laboratory; http://www nndc bnl gov/
145. G Henriksen, P Hoff, R H Larsen *Appl. Radiat. Isot.* **56** 667 (2002)
146. G Henriksen, B W Schoultz, T E Michaelsen, Ø S Bruland, R H Larsen *Nucl. Med. Biol.* **31** 441 (2004)
147. *Directory of Cyclotrons used for Radionuclide Production in Member States. 2006 Update*. IAEA-DCRP/2006, Vienna, 2006
148. S M Deyev, E N Lebedenko, L E Petrovskaya, D A Dolgikh, A G Gabibov, M P Kirpichnikov *Russ. Chem. Rev.* **84** 1 (2015)
149. *Radioimmunotherapy of Cancer* (Eds P G Abrams, A R Fritzberg) (New York, Basel: Marcel Dekker, 2000)
150. J N Bryan, F Jia, H Mohsin, G Sivaguru, W H Miller, C J Anderson, C J Henry, M R Lewis *Nucl. Med. Biol.* **32** 851 (2005)
151. Y Zhou, J D Marks *Methods Enzymol.* **502** 43 (2012)
152. K E Baidoo, K Yong, M W Brechbiel *Clin. Cancer Res.* **19** 530 (2013)
153. R F Meredith, J Torgue, M T Azure, S Shen, S Saddekni, E Banaga, R Carlise, P Bunch, D Yoder, R Alvarez *Cancer Biother. Radiopharm.* **29** 12 (2014)
154. G Vaidyanathan, M R Zalutsky *Curr. Radiopharm.* **4** 283 (2011)
155. V Boudousq, L Bobyk, M Busson, V Garambois, M Jarlier, P Charalambatou, A Pèlegrin, S Paillas, N Chouin, F Quenet, P Maquaire, J Torgue, I Navarro-Teulon, J-P Pouget *PLoS One* **8** e69613 (2013)
156. A A Rosenkranz, G Vaidyanathan, O R Pozzi, V G Lunin, M R Zalutsky, A S Sobolev *Int. J. Radiat. Oncol. Biol. Phys.* **72** 193 (2008)
157. E F Aronsson, J Grétarsdóttir, L Jacobsson, T Bäck, S Hertzman, S Lindegren, B Karlsson, L Lindholm, S Holmberg, L Hafström, S Mattsson *Nucl. Med. Biol.* **20** 133 (1993)
158. B Cornelissen, K A Vallis *Curr. Drug Discov. Technol.* **7** 263 (2010)
159. T A Slastnikova, A A Rosenkranz, M R Zalutsky, A S Sobolev *Curr. Pharm. Des.* **21** 1227 (2015)
160. C Yewale, D Baradia, I Vhora, S Patil, A Misra *Biomaterials* **34** 8690 (2013)
161. P Chen, R Cameron, J Wang, K A Vallis, R M Reilly *J. Nucl. Med.* **44** 1469 (2003)
162. R M Reilly, P Chen, J Wang, D Scollard, R Cameron, K A Vallis *J. Nucl. Med.* **47** 1023 (2006)
163. K A Vallis, R M Reilly, D Scollard, P Merante, A Brade, S Velauthapillai, C Caldwell, I Chan, M Freeman, G Lockwood, N A Miller, B Cornelissen, J Petronis, K Sabate *Am. J. Nucl. Med. Mol. Imag.* **4** 181 (2014)
164. H-W Lo *Translat. Med.* **1** 1000105e (2011)
165. W Han, H-W Lo *Cancer Lett.* **318** 124 (2012)
166. R M Reilly, R Kiarash, R G Cameron, N Porlier, J Sandhu, R P Hill, K A Vallis, A Hendler, J Gariépy *J. Nucl. Med.* **41** 429 (2000)
167. A Fasih, H Fonge, Z Cai, J V Leyton, I Tikhomirov, S J Done, R M Reilly *Breast Cancer Res. Treat.* **135** 189 (2012)
168. Y Yuan, S Chen, T Paunesku, S C Gleber, W C Liu, C B Doty, R Mak, J Deng, Q Jin, B Lai, K Brister, C Flachenecker, C Jacobsen, S Vogt, G E Woloschak *ACS Nano* **7** 10502 (2013)
169. B Hoang, R M Reilly, C Allen *Biomacromolecules* **13** 455 (2012)
170. Y Lu, G N N Mbong, P Liu, C Chan, Z Cai, D Weinrich, A J Boyle, R M Reilly, M A Winnik *Biomacromolecules* **15** 2027 (2014)
171. L Gedda, K Edwards *Tumour Biol.* **33** 661 (2012)
172. L Gedda, A Fondell, H Lundqvist, J W Park, K Edwards *J. Nucl. Med.* **53** 480 (2012)
173. O Sedlacek, M Hruby, M Studenovsky, J Kucka, D Vetvicka, L Kovar, B Rihova, K Ulbrich *Bioconjug. Chem.* **22** 1194 (2011)
174. O Sedlacek, J Kucka, J Mattova, M Parizek, M Studenovsky, M Zadinova, P Pouckova, M Hruby *Eur. J. Pharm. Sci.* **63** 216 (2014)
175. M C Simões, J J Sousa, A A C C Pais *Cancer Lett.* **357** 8 (2015)
176. L Ratkin *Nanoindustry* (2) 26 (2013) [*Nanoindustriya* (2) 24 (2013)]
177. A Müller-Schiffmann, H Sticht, C Korth *BioDrugs* **26** 21 (2012)
178. B B Olsen, H Thisgaard, S Vogel, M Thomassen, T A Kruse, D Needham, J Mollenhauer, P F Høilund-Carlsen *Eur. J. Nanomed.* **5** 181 (2013)
179. R Airley, A Evans *Future Med. Chem.* **4** 2023 (2012)
180. A S Sobolev, D A Jans, A A Rosenkranz *Prog. Biophys. Mol. Biol.* **73** 51 (2000)
181. A A Rosenkranz, A V Ulasov, T A Slastnikova, Yu V Khramtsov, A S Sobolev *Biochemistry (Moscow)* **79** 928 (2014) [*Biokhimiya* **79** 1148 (2014)]
182. A S Sobolev, in *Encyclopedia of Cancer* (Ed. M Schwab) (Berlin, Heidelberg: Springer, 2012) p. 2352
183. Patent US 20130045533 (2013)
184. Patent US 6500800 (2002)
185. A A Rozenkranz, V G Lunin, O V Sergienko, D G Gilyazova, O L Voronina, D E Jans, A A Kofner, M A Shumiantseva, A F Mironov, A S Sobolev *Genetika* **39** 198 (2003) [*Genetika* **39** 259 (2003)]
186. A A Rosenkranz, V G Lunin, P V Gulak, O V Sergienko, M A Shumiantseva, O L Voronina, D G Gilyazova, A P John, A A Kofner, A F Mironov, D A Jans, A S Sobolev *FASEB J.* **17** 1121 (2003)
187. D G Gilyazova, A A Rosenkranz, P V Gulak, V G Lunin, O V Sergienko, Yu V Khramtsov, K N Timofeyev, M A Grin, A F Mironov, A B Rubin, G P Georgiev, A S Sobolev *Cancer Res.* **66** 10534 (2006)
188. A S Sobolev *BioEssays* **30** 278 (2008)

189. A S Sobolev *Biochemistry (Moscow)* **74** 1567 (2009) [*Uspekhi Biol. Khimii* **49** 389 (2009)]
190. A S Sobolev *J. BUON* **14** (Suppl. 1) S33 (2009)
191. T A Slastnikova, A A Rosenkranz, P V Gulak, R M Schiffelers, T N Lupanova, Yu V Khramtsov, M R Zalutsky, A S Sobolev *Int. J. Nanomed.* **7** 467 (2012)
192. Yu V Khramtsov, T I Rokitskaya, A A Rosenkranz, G A Trusov, N V Gnuchev, Y N Antonenko, A S Sobolev *J. Controlled Release* **128** 241 (2008)
193. A A Rosenkranz, Yu V Khramtsov, G A Trusov, N V Gnuchev, A S Sobolev *Dokl. Biochem. Biophys.* **421** 244 (2008) [*Dokl. Akad. Nauk* **421** 835 (2008)]
194. T A Slastnikova, E Koumarianou, A A Rosenkranz, G Vaidyanathan, T N Lupanova, A S Sobolev, M R Zalutsky *EJNMMI Res.* **2** Art. No. 59 (2012)
195. A A Rozenkrants, P A Nabatnikov, R A Aliev, D E Yans, A S Sobolev *Mol. med.* (1) 47 (2004)
196. E Koumarianou, T A Slastnikova, M Pruszynski, A A Rosenkranz, G Vaidyanathan, A S Sobolev, M R Zalutsky *Nucl. Med. Biol.* **41** 441 (2014)
197. T A Slastnikova, A A Rosenkranz, T N Lupanova, P V Gulak, N V Gnuchev, A S Sobolev *Dokl. Biochem. Biophys.* **446** 235 (2012) [*Dokl. Akad. Nauk* **446** 342 (2012)]